# Quantification of potential macroseismic effects of the induced seismicity that might result from hydraulic fracturing for shale gas exploitation in the UK

## Rob Westaway[1,2*] & Paul L. Younger[1]

[1]School of Engineering, University of Glasgow, Glasgow G12 8QQ, UK
[2]Newcastle Institute for Research on Sustainability, Devonshire Building, Newcastle University, Newcastle upon Tyne NE1 7RU, UK
*Corresponding author (e-mail: robert.westaway@glasgow.ac.uk)

**Abstract:** The furore that has arisen in the UK over induced microseismicity from 'fracking' for shale gas development, which has resulted in ground vibrations strong enough to be felt, requires the urgent development of an appropriate regulatory framework. We suggest that the existing regulatory limits applicable to quarry blasting (i.e. peak ground velocities (PGV) in the seismic wavefield incident on any residential property of $10\,mm\,s^{-1}$ during the working day, $2\,mm\,s^{-1}$ at night, and $4.5\,mm\,s^{-1}$ at other times) can be readily applied to cover such induced seismicity. Levels of vibration of this order do not constitute a hazard: they are similar in magnitude to the 'nuisance' vibrations that may be caused by activities such as walking on wooden floors, or by large vehicles passing on a road outside a building. Using a simple technique based on analysis of the spectra of seismic S-waves, we show that this proposed daytime regulatory limit for PGV is likely to be satisfied directly above the source of a magnitude 3 induced earthquake at a depth of 2.5 km, and illustrate how the proposed limits scale in terms of magnitudes of induced earthquakes at other distances. Previous experience indicates that the length of the fracture networks that are produced by 'fracking' cannot exceed 600 m; the development of a fracture network of this size in one single rupture would correspond to an induced earthquake *c*. magnitude 3.6. Events of that magnitude would result in PGV above our proposed regulatory limit and might be sufficient to cause minor damage to property, such as cracked plaster; we propose that any such rare occurrences could readily be covered by a system of compensation similar to that used over many decades for damage caused by coal mining. However, it is highly unlikely that future 'fracking' in the UK would cause even this minor damage, because the amount of 'force' applied in 'fracking' tends to be strictly limited by operators: this is because there is an inherent disincentive to fracture sterile overburden, especially where this may contain groundwater that could flood-out the underlying gas-producing zones just developed. For the same reason, seismic monitoring of 'fracking' is routine; the data that it generates could be used directly to police compliance with any regulatory framework. Although inspired by UK conditions and debates, our proposals might also be useful for other regulatory jurisdictions.

The mechanisms whereby human activities can affect seismicity have been widely discussed in recent years (e.g. Seeber 2002; Westaway 2002, 2006; Klose 2007, 2013; Ellsworth 2013). Following Klose (2013), an 'anthropogenic earthquake' can be defined as any seismic event for which a human activity can reasonably be shown to be the cause, or at least a major influence on event timing. Anthropogenic earthquakes can in turn be subdivided into 'triggered' and 'induced' events; a triggered event is one that would have occurred anyway, because the state of stress in the area was tending towards the condition for shear failure, so that the human activity merely brought the earthquake forward in time or 'advanced the clock'. An earthquake is 'induced' if there is no reason to consider that, in the absence of human activity, the state of stress in the area was heading towards the condition for shear failure: in other words, without the human activity the earthquake would never have occurred. This paper will consider the strength of ground vibrations caused by earthquakes that may be induced by hydraulic fracturing, or 'fracking', for shale gas development. Although tailored towards UK-based issues, it may also be of interest to those responsible for regulating this issue under other jurisdictions, as an alternative to the rather *laissez-faire* approach to regulation that has hitherto applied in the country where this technology was first developed.

The history of 'fracking' as a technology for production of shale gas has been well documented (e.g. Martineau 2007); the much more limited extent of use of 'fracking' in the UK has been summarized by Mair *et al.* (2012) and Younger (2014). 'Fracking' can indeed be regarded as an artificial analogue of natural geological processes involving over-pressured fluids, such as the injection of sills (e.g. Goulty 2005) or clastic dykes (e.g. Van Der Meer *et al.* 2009). The first 'fracking' tests on a shale gas well in the UK took place in early 2011, at Preese Hall near Blackpool, in NW England. This test gave rise to about 50 microearthquakes, concentrated around the *c*. 2.5 km depth of the 'fracking'. Remarkably, given that tens of thousands of boreholes have been used for 'fracking' in the USA without similar outcomes (e.g. Hitzman *et al.* 2013), two of these seismic events were of elevated magnitude: one of local magnitude ($M_L$) 2.3 on 1 April 2011 and another of $M_L$ 1.5 on 27 May 2011 (BGS 2011*a*,*b*). As would be expected, neither of these events caused any surface

damage; they were also not felt by scientific staff at the drilling site (P. Turner, pers. comm.). Only one person claimed to have felt the subsequent $M_L$ 1.5 event. In the ensuing furore, the 'fracking' operations were suspended pending a government investigation. Subsequent studies (De Pater & Baisch 2011; Green *et al.* 2012) established that previously unmapped faults in the vicinity, which must have already been close to the condition for rupture, were brought to this condition by the increase in fluid pressure resulting from the 'fracking'; the timing and location of the induced seismicity leave no doubt that the 'fracking' activities were the cause (Mair *et al.* 2012). The scale of the related media and political fallout cannot be overstated, and has been described as 'hysterical' (Younger 2014). Subsequently, several attempts have been made to propose or recommend guidelines for the magnitude of the ground vibrations induced by 'fracking' that can be deemed acceptable in the UK (e.g. De Pater & Baisch 2011; Green *et al.* 2012; Mair *et al.* 2012; UKOOG 2013), to permit the resumption of development of what may prove to be an important energy resource (see Andrews 2013). However, there has been no consensus between these proposals, which differ markedly from corresponding recommendations for the USA (e.g. Bull 2013), where there is much greater experience of 'fracking' (e.g. Hitzman *et al.* 2013). The recent proposals also fail to take account of the mainstream literature on engineering seismology and earthquake hazards. Although one of the principal conclusions of the Hitzman *et al.* (2013) report by the US Academy of Sciences was indeed that 'The process of hydraulic fracturing a well as presently implemented for shale gas recovery does not pose a high risk for inducing felt seismic events', one looks in vain within this lengthy document for any quantitative recommendation.

The broader context of these debates lies in the energy markets. Heat energy, primarily for heating buildings, has been estimated as 42% of total energy demand for the UK as a whole and, owing to the harsher climate, >50% of the total for Scotland (e.g. IMechE 2011). Some 70% of domestic energy consumption in the UK is from natural gas, most of which is used for heating (e.g. DECC 2013*a*), a pattern that is predicted to continue for the foreseeable future, and will require supply on a large scale. Furthermore, the combined cycle gas turbine (CCGT), in which the hot exhaust from a gas turbine is used to generate steam to power a steam turbine, and both the gas turbine and associated steam turbine drive an alternator, is the most thermally efficient technology for using fossil fuel for electricity generation, overall thermal efficiencies of >60% being achievable (e.g. Bartos 2011). Management of the British national electricity grid includes balancing generation by wind turbines and CCGT plant, the latter providing backup for the former on days with little wind (e.g. Gridwatch 2014). CCGT capacity is thus an essential element of any 'low-carbon' energy strategy for the foreseeable future; hence the production of shale gas offers the potential for significant environmental as well as economic benefits, provided any social and environmental disbenefits can be quantified and managed. In this regard, shale gas does not differ from any other energy conversion technology, be it fossil or renewable. For a broader discussion on the pros and cons of shale gas development, the interested reader is referred to the House of Lords (2014).

How do the concerns over 'fracking'-induced seismicity relate to the wider field of earthquake hazard mitigation? Most work in engineering seismology concerns quantification of hazard from relatively large earthquakes, to mitigate the loss of life and damage to property that can result. In comparison, the extent of past investigations of macroseismic effects of microearthquakes, such as those induced by 'fracking', has been relatively limited, presumably owing to a lack of severe consequences. It should nonetheless be apparent that there is a gradation of effects, as the size of earthquakes and the amplitude of the resulting seismic vibrations decreases, from 'hazard' to 'nuisance'. In turn, some aspects of 'nuisance' ground vibrations, notably those arising from quarry blasting, have a long history of regulation in the UK. On the other hand, other forms of 'nuisance' ground vibration, such as those resulting from people jumping onto hard surfaces or slamming doors, are subject to no legal regulatory framework at all, owing to their essentially trivial character (Table 1). The aims of the present paper are to establish where the observed 'fracking'-induced microseismicity should be placed within this spectrum (ranging from hazard to significant nuisance to trivial nuisance) and to suggest a strategy for the development of the regulatory framework for microseismicity induced by future 'fracking' operations in the UK.

## Conceptual background

In general, 'fracking' may induce seismicity via two general methods (e.g. Šílený *et al.* 2009; Song & Toksöz 2011; Eaton *et al.* 2014; Song *et al.* 2014). First, the 'fracking' fluid may leak into pre-existing faults or fractures in the surrounding rock mass; by increasing the local fluid pressure it may bring such a fault to the condition for shear failure, thus inducing a conventional shear earthquake. Second, the 'fracking' process may directly result in the creation of tensile fractures, associated with the occurrence of earthquakes with tensile mechanisms. 'Mixed-mode' earthquakes, involving both tensile and shear components in variable proportions, are also possible (e.g. Ramsey & Chester 2004; Fojtíková *et al.* 2010). Theory for amplitudes of the resulting seismic waves, based on the established literature on fracture mechanics (e.g. Griffith 1924; Sneddon 1951; Eshelby 1957), which is itself ultimately derived from pioneering studies of the fracturing process such as those by Rankine (1843, 1858), is presented in the Appendix. For conventional shear earthquakes the S-wave usually has larger amplitude than the P-wave; the same is shown to be usually true for tensile fracture earthquakes, at least in rocks of low Poisson's ratio such as Carboniferous mudstones. The ability to form tensile and shear fractures in previously intact rock is determined by the tensile strength $S_T$ and cohesion $S_C$ of the rock, respectively (e.g. Eaves & Jones 1971; Bourne & Willemse 2001); it is likewise also arguable that reactivation of pre-existing faults or fractures is also governed by their cohesion, rather than being a purely frictional process, as fractures may 'heal' following single ruptures (e.g. Reches 1999; Muhuri *et al.* 2003). The stress drop $\Delta\sigma$ that occurs as a result of any earthquake, and that relates to the displacement-to-length ratio $c$ of the associated fault slip or tensile fracture opening, thus depends on $S_C$ or $S_T$. In the analysis presented in the Appendix, therefore, these rock mechanical properties are factored in explicitly.

Earthquake magnitude scales, such as the aforementioned $M_L$, provide an empirical basis for quantifying the 'size' of earthquakes, each being based on the logarithm of the amplitude of seismic waves recorded on a particular type of seismograph located at a standard distance from the seismic source (e.g. Richter 1958). The fundamental physical quantity defining the size of an earthquake is its seismic moment $M_o$, where

$$M_o \equiv \int_S \mu \, u \, ds \qquad (1)$$

$u$ being the coseismic displacement and $\mu$ the shear modulus of the adjoining rock at each point on the seismogenic fault plane of area $s$ (e.g. Keilis-Borok 1959). If, for simplicity, $\mu$ and $u$ are assumed to remain constant across the fault rupture, then $M_o$ can be equated to $\mu\, u\, s$. To facilitate comparison with existing magnitude scales, a 'moment-magnitude' scale, $M_w$, has been defined, thus:

$$\log_{10}\left(M_o \, / \, Nm\right) = 9.05 + 1.5 M_w \qquad (2)$$

**Table 1.** *Amplitudes of ground vibrations that might cause hazard or nuisance*

| Item | Amplitude (mm s$^{-1}$) | Reference |
|---|---|---|
| Threshold for major damage | 60 | 1 |
| Threshold for plaster cracking | 50 | 2 |
| 600 m × 600 m vertical fracture initiated at 2.5 km depth in Carboniferous mudstone ($M_W$ 3.6) | *c.* 50 | 3 |
| Threshold for minor damage at Modified Mercalli Intensity V | 34 | 4 |
| Threshold for cosmetic damage | 15 | 1 |
| 'Safe' limit | 12.7 | 5 |
| Slamming door | 12.7 | 6 |
| Upper limit for quarry blasting during the working day (allowable if unavoidable) | 10 | 7 |
| Jumping onto a wooden floor | 8 | 6 |
| Upper limit for quarry blasting during the working day (desirable) | 6 | 7 |
| Upper limit for quarry blasting during daytime outside the working day | 4.5 | 7 |
| Upper limit for quarry blasting at night | 2 | 7 |
| Lorry at a distance of *c.* 8 m | 2 | 8 |
| Threshold for felt effect at Modified Mercalli Intensity II | 1 | 4 |
| Walking on a wooden floor | 0.8 | 6 |
| DECC (2013*b*) limit for suspension of fracking ($M_W = 0.5$ tensile earthquake) at 2.5 km depth | *c.* 0.4 | 3 |
| Minimum threshold of perception for ground vibrations caused by blasting | 0.25 | 9 |
| Minimum threshold of perception for ground vibrations caused by road traffic | 0.15 | 10 |

Reference codes: 1, BS7385-2 (BSI 1993); 2, Calder (1977); 3, predictions from this study, which include radiation pattern effects, but for reasons discussed in the text are probably overestimates; 4, Wald *et al.* (1999); 5, Siskind *et al.* (1980); 6, Stagg *et al.* (1980); 7, BS6472-2 (BSI 2008); 8, NCHRP (1999); 9, Oriard (1972, 2002); 10, Whiffen & Leonard (1971).

(Hanks & Kanamori 1979), equivalent to

$$M_w = \frac{2}{3}\left[\log_{10}\left(M_o / Nm\right) - 9.05\right]. \qquad (3)$$

Without explicitly stating so, the analyses by De Pater & Baisch (2011) and Green *et al.* (2012) have assumed that the reported $M_L$ values for the 'fracking'-induced microearthquakes in the UK equate to $M_w$, and so can be converted into $M_o$. To facilitate comparison with their work, we will make the same assumption; this allows the reported magnitudes to be related to a substantial body of theory and empirical evidence, although it should be noted that many earthquakes induced by 'fracking' have tensile fracture focal mechanisms and thus differ from the double-couple mechanisms characteristic of 'conventional' earthquakes that occur as a result of shearing across faults (e.g. Walter & Brune 1993; Shi & Ben-Zion 2009; Eaton *et al.* 2014); some of the consequences of such differences become apparent during the course of our analysis.

Theory relating to elastic stresses and associated seismic radiation from a circular fracture of radius *a*, which opens in rock of Poisson's ratio ν as a result of a uniform excess internal pressure *P*, is presented in the Appendix. Combining one of these equations (equation (A11)) with equation (2) gives a simple scaling relation linking $M_w$, *a*, ν, and *P*:

$$\log_{10}\left(a\right) = \left[9.05 - \log_{10}\left(8/3\right)\right]/3 \\ + 0.5\,M_w - \log_{10}\left(P\right)/3 - \log_{10}\left(1-\nu\right)/3 \qquad (4)$$

with *a* in metres and *P* in pascals. Eaton *et al.* (2014) derived a similar equation but their analysis utilized a different relation between $M_w$ and $M_o$ and also incorporated the unstated assumption that ν = 0.25. Equation (4) demonstrates that there is a clear link between the 'fracking' procedure in operation, represented by *P*, the dimensions of the fractures produced (represented by *a*), the magnitudes of the resulting earthquakes (represented by $M_w$), and the physical properties of the rock mass that is being 'fracked' (represented by ν). Thus, for example, with *P* = 1 MPa and ν = 0.2, if an $M_w = 0.5$ earthquake occurs as a result of the creation of a new circular fracture, this fracture will have a

predicted radius of *c.* 14 m. However, such analysis does not make any deterministic prediction of the amplitude of the ground vibrations expected for induced earthquakes of any size; more elaborate investigation is evidently needed.

Looking at the mechanics in more detail, we assume once again that microearthquakes rupture circular patches of fault with radius *a*, such that

$$M_o = \pi\mu a^2 U \qquad (5)$$

where *U* is the spatial average coseismic slip. For a circular fault, the static stress drop Δσ can be determined (e.g. Lay & Wallace 1995) as

$$\Delta\sigma = \frac{7\pi}{16}\mu\frac{U}{a} = \frac{7\pi}{16}\mu c \qquad (6)$$

where *c* = *U*/*a* is the ratio of average displacement to radius of the fault. Combining equations (5) and (6) thus gives, for a circular fault, the standard expression

$$\Delta\sigma = \frac{7M_o}{16a^3}. \qquad (7)$$

However, the standard derivation of this formula (like many others in this field) has included the assumption that the faulting is in rock with a Poisson's ratio ν = 0.25; for the general case it adjusts (see the Appendix, equation (A20)) to

$$\Delta\sigma = \frac{3\,(2-\nu)M_o}{16\,(1-\nu)a^3}. \qquad (8)$$

Equation (6) likewise adjusts to

$$\Delta\sigma = \frac{3\,(2-\nu)\pi}{16\,(1-\nu)}\mu c. \qquad (9)$$

The energy radiated by an earthquake source in the form of seismic waves, $E_s$, can also be estimated, after Kanamori (1977), as

$$E_s = \frac{\Delta\sigma\, M_o}{2\mu}. \qquad (10)$$

Many studies (e.g. Ide & Beroza 2001; Allmann & Shearer 2009) have shown that across many orders of magnitude of $M_o$, earthquakes maintain constant stress drops $\Delta\sigma$ in the range $c.$ 1–10 MPa (typically $c.$ 3 MPa) and, although exceptions have been noted (e.g. Archuleta et al. 2012), constancy of stress drop (or constancy of the ratio of coseismic slip to the dimensions of the seismogenic fault) is generally regarded as the key basis for the scaling behaviour of earthquakes (e.g. Shaw 2009).

Furthermore, theory (e.g. Aki 1967; Brune 1970) indicates that the spectral amplitude of the particle displacement for seismic S-waves (which usually produce the strongest ground vibrations near any earthquake source) radiated by an earthquake is flat at frequencies $f$ below the corner frequency $f_c$ (at a low-frequency asymptote $\Omega^s$ given by

$$\Omega^s = \frac{R_{\theta\phi} M_o}{4\pi\rho v_s^3 R} \qquad (11)$$

where $R_{\theta\phi}$ is the directional coefficient for the S-wave radiation pattern, $\rho$ and $v_s$ are the density and S-wave velocity of the rock adjoining the fault, and $R$ is distance from the source), but decreases rapidly (as $c.\ f^{-2}$) for $f \gg f_c$. This theory was originally developed for conventional double-couple seismic sources, representing shear fractures; however, as is discussed in the Appendix, similar formulae are applicable for both P- and S-waves radiated either by shear fractures or by tensile fractures. It follows that the spectral velocity amplitude increases in proportion to $f$ for $f < f_c$ but decreases as $c.$ $f^{-1}$ for $f \gg f_c$. The strongest velocities of ground motion produced by an earthquake will thus be at frequencies around $f_c$. Theoretical models predict that for a circular earthquake source of radius $a$

$$f_c = \frac{\Lambda_s v_s}{2\pi a} \qquad (12)$$

where $\Lambda_S$ is a dimensionless factor; for example, for the Brune (1970) source model, $\Lambda_S \approx 2.34$. However, as is discussed in the Appendix, for a given seismic event $f_c$ may be higher for P-waves than for S-waves. Furthermore, the root mean square angular average of $R_{\theta\phi}$ for tensile fracture events is higher for the P-wave than for the S-wave (from Walter & Brune 1993, it is $\sqrt{(47/15)}$ for the P-wave, in rock with a Poisson's ratio of 0.25, and $\sqrt{(8/15)}$ for the S-wave), whereas for shear fracture events the reverse is true ($\sqrt{(4/15)}$ and $\sqrt{(6/15)}$, respectively; e.g. Aki & Richards 1980, p. 120). In addition, the S-wave radiation pattern for a tensile fracture earthquake has nodal directions, along which the amplitude of the radiated wave is zero, whereas P-waves are radiated in all directions (e.g. Shi & Ben-Zion 2009). Each of these factors will result in stronger P-waves than S-waves, although this effect is offset by presence of $v_p^3$ rather than $v_s^3$ in the denominator of the P-wave version of equation (11). Overall, the amplitudes of P-waves relative to S-waves are thus expected to be higher for tensile fracture earthquakes than for shear earthquakes, thereby providing a standard method for identifying the former (or for determining the relative contributions of tensile and shear deformations for 'hybrid' events) (e.g. Walter & Brune 1993; Ramsey & Chester 2004; Šílený et al. 2009; Song & Toksöz 2011; Vavryčuk 2011; Kwiatek & Ben-Zion 2013; Eaton et al. 2014; Song et al. 2014). However,

even so, the Appendix shows that the S-wave radiated by a tensile fracture earthquake will usually be stronger than the P-wave, especially in rocks with a low Poisson's ratio.

One long-standing approach to the quantification of macroseismic effects has been via empirical prediction equations for either peak ground acceleration or peak ground velocity. Historically, in engineering seismology, felt effects and damage were generally related to peak ground acceleration; however, in recent years, peak ground velocity (PGV) has been perceived as an appropriate proxy in many circumstances (e.g. Wald et al. 1999; Wu et al. 2004; Bommer & Alarcón 2006; Akkar & Bommer 2007). Such empirical predictions are nonetheless subject to considerable variability, in part owing to different approaches to quantifying earthquake sources, such as specifying the limits of any fault plane (e.g. Westaway & Smith 1989). Prediction of PGV or peak ground acceleration for microearthquakes, for which the dimensions of the fault plane will be small compared with source–station distances, is likewise subject to considerable variability, not least because relatively few prediction equations have been calibrated for these small events, so what constitutes a 'reasonable prediction' has not previously been straightforward to ascertain (e.g. Bommer et al. 2007). Figure 1 illustrates the predictions for peak horizontal and vertical ground velocity at zero epicentral distance $d$, corresponding to a point on the Earth's surface directly above an earthquake source, for one prediction equation, from Bragato & Slejko (2005), which has been calibrated down to magnitude 2.5. For example, for $M_L$ 4, the resulting predictions of PGV are 21 mm s$^{-1}$ (vertical) and 7 mm s$^{-1}$ (horizontal). However, this prediction equation does not explicitly incorporate the depth $h$ of any seismic source; its predictions depend on a distance parameter $x = \sqrt{(d^2 + k^2)}$ where $k$ is an empirical constant (specified as 7.3 km and 9.1 km, respectively, for the vertical and horizontal components) that effectively limits the magnitude of the prediction as $d \to 0$. Because the depth of the observed induced seismicity ($c.$ 2.5 km) is rather less than this, these predictions can be expected to underestimate the ground velocities that are actually anticipated. To overcome this effect, one might 'doctor' the prediction equations by setting $x = 2.5$ km; the (much higher) predictions that result (e.g. PGV $c.$ 200 mm s$^{-1}$ for magnitude 4) are also indicated in Figure 1.

Another long-standing method for prediction of macroseismic effects has been through stochastic modelling, in which earthquake-induced ground vibrations are simulated by treating the seismic source as a combination of oscillators of random phase, distributed with appropriate amplitude ranges across an appropriate frequency range, with effects of geometrical spreading and anelastic attenuation also factored in (e.g. Boore 2003; Boore & Thompson 2012). Boore (2003) illustrated such a simulation for a magnitude 4 event at a distance of 10 km, in which the PGV was calculated as 6.1 mm s$^{-1}$, the strongest spectral velocity components being $c.$ $f = 8$ Hz. Scaling for geometrical spreading would increase this prediction to 24.4 mm s$^{-1}$ at 2.5 km distance. Correction for anelastic attenuation can also be made using the standard equation

$$A = A_o \exp\left[ -\pi R f / (Q v_s) \right] \qquad (13)$$

(e.g. Toksöz & Johnston 1981), where $A_o$ and $A$ are the amplitudes of a seismic wave of frequency $f$ before and after correction for propagation for a distance $R$ through a medium with S-wave velocity $v_s$ and anelastic quality factor $Q$. Taking $Q = 500$ for $f = 8$ Hz, and $v_s = 3500$ m s$^{-1}$ (Boore 2003), one arrives at a PGV prediction at 2.5 km distance from a magnitude 4 event of $c.$ 27 mm s$^{-1}$. This prediction is thus somewhat higher than those obtained by direct use of the Bragato & Slejko (2005) empirical prediction equations but much lower than those obtained for $x = 2.5$ km using the 'doctored' versions of their equations. For comparison, in a discussion of
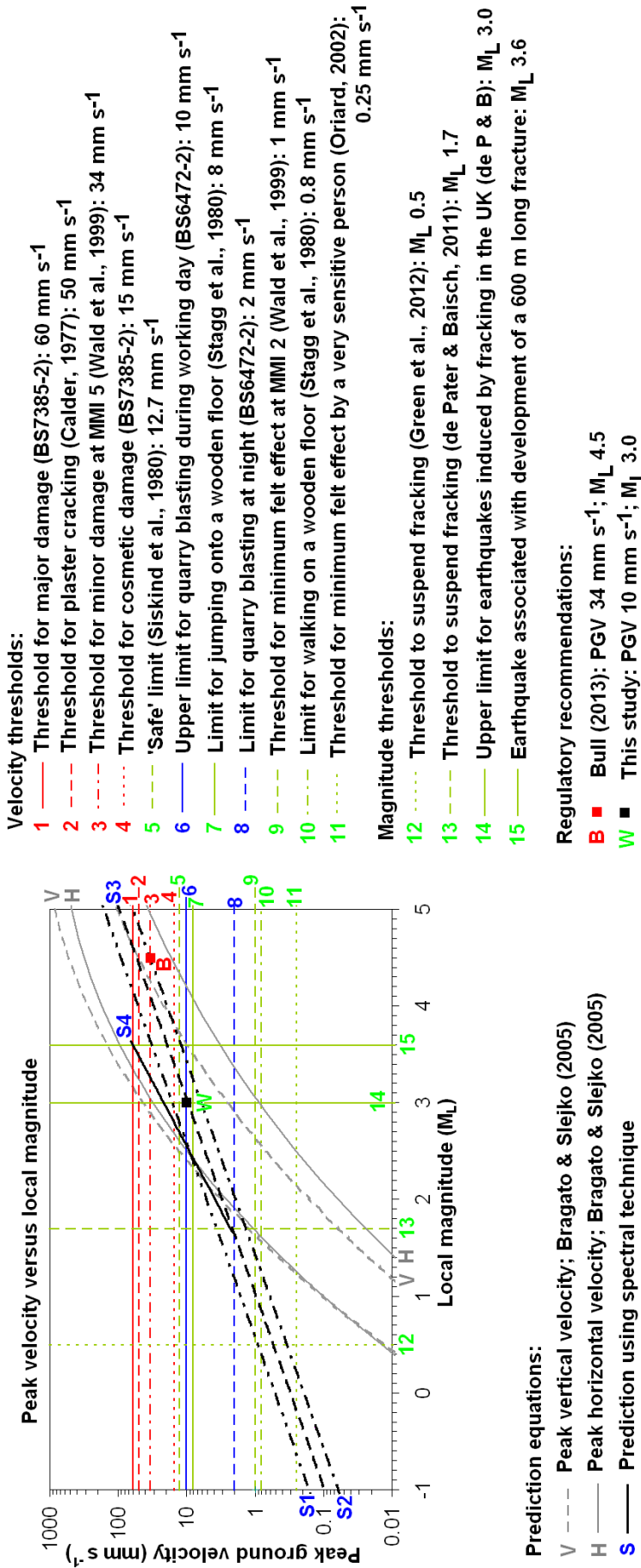
**Fig. 1.** Comparison of regulations for peak ground velocity at residential property from quarry blasting, applicable in the UK, with felt effects, proposed magnitude thresholds for regulating 'fracking' in the UK, estimates of PGV from various other forms of environmental nuisance, and predictions of vertical and horizontal PGV from Bragato & Slejko (2005) and from the spectral method developed in this study. All predictions are for points on the Earth's surface directly above 'fracking' at a depth of 2.5 km, so $R = 2.5$ km; the two sets of predictions after Bragato & Slejko (2005) correspond to the original (lower) and 'doctored' (higher) versions of their equations, both versions being calibrated for $M_L \geq 2.5$ and extrapolated to lower magnitudes for illustrative purposes only. All predictions for the spectral method developed in this study assume $\mu = 12.7$ GPa, $v = 0.18$, $\rho = 2550$ kg m$^{-3}$, $v_s = 2.15$ km s$^{-1}$, $b = 1.6$, $\eta = 0.5$, and $\Phi = 2$, and use equation (3) to determine $M_W = M_L$ from $M_o$. Those for small circular shear fractures (prediction S1; based on equation (A45) assume $S = S_C = 4$ MPa and $m = 2$ (so $B = 0.7$); those for small circular tensile fractures (equation (A49) assume $P = S_T = 2$ MPa and $m = 2$ (so $B = 0.7$; prediction S2) or $m = 4$ (so $B = 1.4$; prediction S3). Those for large, square (i.e. $L = H$), vertical tensile fractures assume $K = 15500$ Pa m$^{-1}$ and $m = 4$ (so $B = 1.4$) to determine $M_o$ from $H$, then equation (A54) to determine PGV (prediction S4). Other estimates of the magnitudes of 'nuisance' vibrations correspond to those depicted; thus, for example (Table 1), PGV may reach 12.7 mm s$^{-1}$ from a slamming door (Stagg et al. 1980) or 2 mm s$^{-1}$ from a lorry at a distance of c. 8 m (NCHRP 1999).

**Peak velocity versus local magnitude**

**Velocity thresholds:**

1 — Threshold for major damage (BS7385-2): 60 mm s⁻¹
2 — — Threshold for plaster cracking (Calder, 1977): 50 mm s⁻¹
3 — · — Threshold for minor damage at MMI 5 (Wald et al., 1999): 34 mm s⁻¹
4 ····· Threshold for cosmetic damage (BS7385-2): 15 mm s⁻¹
5 — — 'Safe' limit (Siskind et al., 1980): 12.7 mm s⁻¹
6 — Upper limit for quarry blasting during working day (BS6472-2): 10 mm s⁻¹
7 — Limit for jumping onto a wooden floor (Stagg et al., 1980): 8 mm s⁻¹
8 — — Limit for quarry blasting at night (BS6472-2): 2 mm s⁻¹
9 — · — Threshold for minimum felt effect at MMI 2 (Wald et al., 1999): 1 mm s⁻¹
10 — · · — Limit for walking on a wooden floor (Stagg et al., 1980): 0.8 mm s⁻¹
11 ····· Threshold for minimum felt effect by a very sensitive person (Oriard, 2002): 0.25 mm s⁻¹

**Magnitude thresholds:**

12 ····· Threshold to suspend fracking (Green et al., 2012): $M_L$ 0.5
13 — — Threshold to suspend fracking (de Pater & Baisch, 2011): $M_L$ 1.7
14 — Upper limit for earthquakes induced by fracking in the UK (de P & B): $M_L$ 3.0
15 — Earthquake associated with development of a 600 m long fracture: $M_L$ 3.6

**Regulatory recommendations:**

B ■ Bull (2013): PGV 34 mm s⁻¹; $M_L$ 4.5
W ■ This study: PGV 10 mm s⁻¹; $M_L$ 3.0

**Prediction equations:**

V — — Peak vertical velocity; Bragato & Slejko (2005)
H — Peak horizontal velocity; Bragato & Slejko (2005)
S — Prediction using spectral technique

regulatory limits for 'fracking', Bull (2013) estimated that an induced earthquake of $M_L$ 4.5 would have a PGV of $c.$ 34 mm s$^{-1}$.

This stochastic modelling approach has not previously been applied to quantification of the hazard (or nuisance) caused by the microseismicity induced by 'fracking' in the UK. Pending a formal analysis of this type, a simpler approach will be provided here. Thus, if it is assumed that all frequency components radiated by the earthquake source oscillate in phase (rather than having random phase relations) with spectral displacement amplitudes as described above (i.e. constant at $\Omega$ (equation (11)) for $f \leq f_c$ and proportional to $f^{-2}$ for $f > f_c$, up to some limiting frequency $mf_c$) and anelastic attenuation is neglected, the peak ground velocity $v_{max}$ can be evaluated as described in the Appendix as

$$v_{max} = \pi\ \Phi\ \Omega\ f_c{}^2(1 + 2B) \qquad (14)$$

where $B = \ln(m)$, $\Omega$ might be $\Omega^{SP}$, $\Omega^{SS}$, $\Omega^{TP}$, or $\Omega^{TS}$ (see Appendix), depending on whether one is considering P- or S-waves radiated by a shear or tensile earthquake source, and $\Phi$ is the free-surface amplification factor for this type of seismic wave (see also the Appendix). As already noted, the Appendix also demonstrates that the familiar property of shear earthquakes, that the S-wave is typically stronger than the P-wave, is also usually the case for tensile earthquakes as well, especially in rocks of low Poisson's ratio. Hence, our analysis of PGV from 'fracking' concentrates on the amplitudes of S-waves; the resulting equations are stated in full in the Appendix (equations (A46) and (A50), respectively, for S-waves from shear and tensile earthquakes).

Figure 1 shows predictions on this basis, with $R_{\theta\varphi}$ taken as its maximum value of unity and with $\Phi = 2$ (see Appendix), for shear earthquakes for $m = 2$, such that $B \approx 0.7$, and for tensile earthquakes for $m = 2$, such that $B \approx 0.7$, and for $m = 4$, such that $B \approx 1.4$, in each case at a distance of 2.5 km. The first of these predictions indicates $v_{max} = 52$ mm s$^{-1}$ for $M_L$ 4, somewhat in excess of the stochastic prediction derived from Boore (2003). This difference is partly a reflection of differences in method (e.g. Boore (2003) factored in anelastic attenuation and assumed an angular average of the radiation pattern, whereas for this calculation we have not considered any effect of anelastic attenuation and have assumed the maximum of the radiation pattern in every direction; there are also differences in the approaches regarding calculation of the corner frequency and different choices of rock properties). Furthermore, generations of seismological studies (e.g. Aki 1969; Aki & Chouet 1975; Frankel & Clayton 1986; Frankel & Wennerberg 1987; Sato & Fehler 1998; Gao et al. 2013) have established that scattering of seismic waves by heterogeneities transfers energy from direct seismic phases into other phases that arrive later, reducing the amplitude of the direct phases. By neglecting any effect of scattering our analysis will thus overestimate the amplitude of the expected seismic ground vibrations. In addition, any prediction using equation (14) is also likely to overestimate the true PGV because in reality the different frequency components of any earthquake source will not be in phase (and so will partly cancel one another) and because anelastic attenuation (cf. equation (13)) will be significant, especially at high frequencies. Conversely, to match the much higher PGV predictions derived from the 'doctored' use of the Bragato & Slejko (2005) prediction equation ($h$ set to zero and $x = 2.5$ km), much higher values of $B$ would be necessary. Alternative predictions on this basis, not illustrated in Figure 1, would require very high values of $m, c.$ $10^{13}$, which would require significant contributions to $v_{max}$ from very high frequencies of ground motion that would be physically implausible were anelastic attenuation to be taken into consideration. Figure 1 also indicates that for a given $M_L$, tensile earthquakes are predicted to cause significantly smaller PGV than for shear earthquakes. As is discussed in the Appendix, this distinction arises from differences in the underlying source mechanics,

being due in part to the dependence of the predictions on different rock properties and in part to their different angular variations in seismic radiation. The predictions scale in relation to the parameter $S$, the initial shear stress in the adjoining rock mass, for shear earthquakes, and $P$, the excess fluid pressure, for tensile earthquakes. Our calculations incorporate the assumptions that for fracturing to occur $S$ will be equivalent to the cohesion ($S_C$) of the rock mass, and $P$ to its tensile strength ($S_T$). Part of the basis for our prediction of larger PGV for shear earthquakes is that $S_C > S_T$; even if these quantities were set equal to one another, however, the differences between the seismic radiation patterns would still result, for a given value of $m$, in the prediction of larger PGV for shear earthquakes. Furthermore, strictly speaking, the independent variable used in our predictions in Figure 1 is, in effect, $M_o$, not $M_L$; in the analysis to produce these predictions, $M_o$ has been converted to $M_W$ using equation (3), and the resulting values of $M_W$ are assumed (as already stated) equivalent to $M_L$. However, the realization that shear earthquakes and tensile earthquakes of a given seismic moment will produce systematically different PGV values suggests that, in reality, these two types of earthquake will have different $M_o$–$M_L$ relations. This is one reason why it is undesirable to base regulation of 'fracking' on any threshold for $M_L$, and why it is therefore preferable to use felt effects, expressed as PGV, instead.

## Application to the induced seismicity from 'fracking' in the UK

An initial requirement before any of the theory discussed above can be applied to assess the potential nuisance caused by 'fracking' in the UK is to constrain the relevant physical properties for the lithologies present. However, there is relatively little quantitative information on such properties for lithologies that might be subjected to 'fracking' in Britain. Waltham (2009, p. 48) listed as 10 GPa and 2300 kg m$^{-3}$ the typical Young's modulus and density of 'Carboniferous mudstone' that might represent the Bowland Shale. With a Poisson's ratio $\nu$ of 0.2, the former value would indicate $\mu$ $c.$ 4.2 GPa (equation (A3)), so equation (A1) would indicate $v_s$ $c.$ 1.35 km s$^{-1}$ and, with $\Delta\sigma = 3$ MPa, equation (9) would give $c$ $c.$ $5 \times 10^{-4}$. Carter & Mills (1976) had previously determined 2–14 GPa for the Young's modulus, 1–8 MPa for the tensile strength $S_T$ and 2–12 MPa for the cohesion $S_C$, for no more than 24 samples of Middle Carboniferous (Namurian) age mudstone from sites in NE England, which might represent analogues for the Bowland Shale. We thus adopt 4 MPa and 2 MPa as representative values of $S_C$ and $S_T$ for this lithology. Significant variability in properties is nonetheless indicated; with such limited sampling it is apparent that these choices are subject to considerable uncertainty.

To avoid any risk of systematic errors arising in our work as a result of using such a limited set of data values, we base our analysis instead on the physical properties of the Barnett Shale. This is a mudstone of Mississippian (i.e. Carboniferous) age that is widespread in the Fort Worth area of Texas and was the first deposit to be developed as a shale gas resource (e.g. Martineau 2007). An abundance of data is therefore available for it, including the following representative properties, which we have taken from Varga et al. (2012) and which are all mutually consistent given equations (A1), (A3), (A4), and (A5): $E$ $c.$ 30 GPa; $\rho$ $c.$ 2550 kg m$^{-3}$; $Z_p$ $c.$ 31000 g cm$^{-3} \times$ ft s$^{-1}$   or   $c.$ $9.45 \times 10^6$ kg m$^{-2}$ s$^{-1}$;   $Z_s$   $c.$ 19400 g cm$^{-3} \times$ ft s$^{-1}$ or $c.$ $5.91 \times 10^6$ kg m$^{-2}$ s$^{-1}$; $\nu$ $c.$ 0.18; $\mu$ $c.$ 12.7 GPa; $v_p$ $c.$ 3.44 km s$^{-1}$; $v_s$ $c.$ 2.15 km s$^{-1}$. Others have reported somewhat different values; for example, Agarwal et al. (2012) quoted $E = 45$ GPa and $\nu = 0.2$, whereas Song et al. (2014) gave $v_p = 4.11$ km s$^{-1}$, $v_s = 2.44$ km s$^{-1}$, and $\rho = 2500$ kg m$^{-3}$. With $S_C = 4$ MPa (see above) and $\nu$ $c.$ 0.18, $E = 30$ GPa would imply, from equation (9), $c$ $c.$ $2.4 \times 10^{-4}$, whereas $E = 45$ GPa would give $c$ $c.$

$1.6 \times 10^{-4}$. Our analysis also requires $S_T$; however, this quantity exhibits considerable variability and is thus subject to some uncertainty. For example, Gale & Holder (2008) reported values ranging from 12 to 44 MPa, whereas Tran *et al.* (2010) reported values between *c.* 1.4 MPa (i.e. 200 p.s.i.) and *c.* 21 MPa (i.e. 3000 p.s.i.). It would indeed appear from these and other studies that Carboniferous mudstones typically consist of relatively weak zones with $S_T$ *c.* 2 MPa, which are most likely to fracture, interspersed with zones where $S_T$ is an order of magnitude larger.

Taking the above theory into account, assuming $\Delta\sigma = S_C = 4$ MPa, $\mu = 12.7$ GPa, and $\nu = 0.18$, so $c \approx 2.4 \times 10^{-4}$, the induced Preese Hall earthquake with $M_L = 2.3$ is predicted to have had $M_o$ *c.* $3 \times 10^{12}$ N m (equation (3)) and to have involved *c.* 17 mm of slip on a fault plane of radius *c.* 70 m and area *c.* 14000 $m^2$ (equation (8)). It released *c.* 500 MJ of energy in the form of seismic waves (equation (10)), with the strongest ground velocities at estimated frequencies (*c.* $f_c$) of *c.* 11 Hz (equation (12), assuming $v_s = 2.15$ km s$^{-1}$). The subsequent $M_L$ 1.5 event had $M_o$ *c.* $2 \times 10^{11}$ N m and involved *c.* 7 mm of slip on a fault plane of radius *c.* 30 m and area *c.* 2000 $m^2$, releasing *c.* 30 MJ of energy as seismic waves with the strongest ground velocities around *c.* 27 Hz. For comparison, detonation of a standard *c.* 200 g stick of dynamite would release *c.* 1 MJ of energy; it is common practice to use *c.* 100 kg of explosive in single quarry blasts in the UK, thus releasing *c.* 500 MJ of energy. According to BGS (2011*a*) the $M_L = 2.3$ event caused no damage but was felt at 23 locations and was assigned an epicentral intensity of IV on the European Macroseismic Scale (EMS). From Figure 1, the PGV in its epicentral area, predicted by our method, was unlikely to have exceeded 7 mm s$^{-1}$. BGS (2011*b*) reported that the $M_L = 1.5$ event also caused no damage but was felt by at least one person (it occurred in the middle of the night when ambient levels of ground vibration would have been low) and was assigned an EMS epicentral intensity of III. From Figure 1, our method predicts that the PGV in its epicentral area may have reached 3 mm s$^{-1}$. Nonetheless, this instance, of two earthquakes large enough to be felt being induced by the 'fracking' of a single well, contrasts markedly with US experience. Thus, as Hitzman *et al.* (2013) noted, up to 2011 some 35000 wells in the USA had been 'fracked' but only one induced earthquake large enough to be felt had been reported; this was of $M_L$ 2.8, and occurred on 18 January 2011 as a result of 'fracking' at *c.* 3 km depth to stimulate oil production at Eola, Oklahoma (Holland 2011). Scaling Figure 1 for the different source depth, our method predicts that this event might have produced a PGV of *c.* 11 mm s$^{-1}$. This discrepancy may have something to do with the fact that US landowners own the mineral rights beneath their property whereas those in the UK do not. On the other hand, according to Mair *et al.* (2012), some 200 onshore wells in the UK have been 'fracked' for purposes other than shale gas production (such as improving oil recovery), with no record of any induced microearthquake having been felt. The largest ever earthquake that is generally accepted as having been induced by 'fracking' occurred on 19 May 2011 in the Horn River Basin, near the town of Fort Nelson in NE British Columbia, Canada. It had $M_L$ 3.8 and was felt but caused no damage (BCOGC 2012); it was considered equivalent to $M_W$ 3.6 by Ellsworth (2013). Nonetheless, other activities in the USA have been associated with much larger earthquakes that have arguably been induced (e.g. Ellsworth 2013; Kerr 2013; Van Der Elst *et al.* 2013); for example, wastewater injection into a borehole at Prague, Oklahoma, was associated with significant seismicity, including an event of $M_w$ 5.7 on 6 November 2011 (Keranen *et al.* 2013).

De Pater & Baisch (2011) estimated the maximum size of any 'fracking'-induced microearthquake in the UK as $M_L$ *c.* 3, based on long-standing experience of mining-induced seismicity (see Kusznir *et al.* 1980; Bishop *et al.* 1993; Donnelly 2006), although Mair *et al.* (2012) suggested a limit of $M_L$ 4 without clear explanation. Subsequently, Fisher & Warpinski (2012) reported an abundance of

observational data indicating that fractures created by 'fracking' may grow to lengths of *c.* 600 m. Davies *et al.* (2012) likewise proposed that the maximum vertical extent of a fracture that can develop as a result of 'fracking' is *c.* 600 m, although natural fracture systems are known with lengths of up to *c.* 1000 m (e.g. Geiser *et al.* 2012; Davies *et al.* 2013; Lacazette & Geiser 2013). As Fisher & Warpinski (2012) explained, fractures induced by 'fracking' will tend to develop upwards because the 'fracking' fluid is less dense than the surrounding rock, so if the conditions at the point of initiation favour the creation of a fracture then the conditions at a slightly shallower depth will exceed the failure criterion for the initial development of the fracture to a greater extent, so the fracture can propagate. However, such propagation is ultimately limited by the excess pressure in the 'fracking' fluid and by the volume of this fluid that is available; the reported *c.* 600 m size limit is thus a reflection of operating practices at the US 'fracking' sites that provided the data for Fisher & Warpinski (2012). Assuming the same set of rock properties as before, including $\mu = 12.7$ GPa, $\nu = 0.18$, and $\rho = 2550$ kg m$^{-3}$, if the vertical stress is lithostatic (such that the parameter $K$ in equation (A30) is *c.* 15500 Pa m$^{-1}$), then the minimum excess pressure in the 'fracking' fluid, required to create such a large fracture, would be *c.* 2.3 MPa (equation (A30)) and the minimum volume of 'fracking' fluid, required to keep the fracture open and allow it to reach this size, would be *c.* 25000 $m^3$ (equation (A32)). If such a large fracture formed in a single rupture, the resulting earthquake would have $M_o$ *c.* $3 \times 10^{14}$ N m (equation (A34)), corresponding to $M_w$ *c.* 3.6 (equation (3)). With this set of parameter values, and again assuming $R_{\theta\phi} = 1$, our prediction method (equation (A54)) would suggest a PGV of *c.* 65 mm s$^{-1}$ at the Earth's surface directly above the fracture, at a distance of 2.5 km (Fig. 1). However, the S-wave radiation pattern for a vertical tensile fracture would have $R_{\theta\phi} = 0$ in the vertical direction (see Appendix), so the actual amplitude of the direct S-wave that travels in this direction will in fact be zero. The maximum amplitude of this direct S-wave will instead be expected at points for which the ray inclination is *c.* 35° to the vertical (see the Appendix; equation (A58)); in this direction $R_{\theta\phi} \approx 0.94$ and the path length for a 2.5 km deep source will be *c.* 3.1 km, so the prediction of PGV decreases to *c.* 50 mm s$^{-1}$ (equation (A54)). Even this prediction will exceed the likely true PGV that would result from the (very unlikely) event of a fracture of this size forming in a single rupture, because the method assumes all frequency components in the seismic S-wave will be in phase (as was noted above, others have estimated that the PGV for induced earthquakes of roughly this size would be *c.* 30 mm s$^{-1}$ rather than *c.* 50 mm s$^{-1}$). This eventuality is anyway amenable to regulation; imposing a tighter regulatory limit on the pressure and/or volume of the 'fracking' fluid would force a lower limit for this 'worst case scenario' prediction.

We note in passing that gas contamination of drinking water wells has been reported near shale gas extraction sites in the USA (e.g. Osborn *et al.* 2011; Jackson *et al.* 2013) and that such evidence has been cited by environmental groups and in the media (e.g. Fox 2010) as evidence that the fracture networks produced by 'fracking' may be much more extensive than the evidence in the previous paragraph would suggest. However, subsequent work indicates that this contamination has nothing directly to do with 'fracking' but is caused instead by defects such as leaking well casing or faulty cementation in the annulus outside the well casing (Darrah *et al.* 2014).

De Pater & Baisch (2011) proposed that future 'fracking' operations should be permitted in the UK subject to real-time seismic monitoring, with work being allowed to proceed with caution should any event above $M_L$ 0.0 occur, but that it should be suspended if any event as large as $M_L$ 1.7 were to occur. However, Green *et al.* (2012) regarded the latter limit as insufficiently cautious and recommended a lower threshold of $M_L$ 0.5 for the suspension of 'fracking'. Mair *et al.* (2012) noted that one of these recommendations was much more conservative than the other but declined to adjudicate. Guidelines for future 'fracking' operations,

issued subsequently by industry practitioners (UKOOG 2013), recognized that other industrial processes that generate vibration, such as quarry blasting, are regulated within the UK on the basis of thresholds of ground velocity or acceleration (rather than $M_L$), and 'fracking' should be analogously regulated with corresponding thresholds.

Guidelines for the allowable amplitudes of ground vibrations induced by quarry blasting are indeed currently provided for the UK by British Standards (BS) 6472 part 2 (BSI 2008) and 7385 part 2 (BSI 1993). BS6472-2 is primarily concerned with quantifying the peak ground velocity $v_{max}$ that can be anticipated at a given distance $d$ from the detonation of a mass $m$ of explosive; it predicts that, with a 10% probability of exceedence,

$$v_{max} = am^b d^{-2b} \qquad (15)$$

where $b = 1.227$ and $a = 168700$ to give $v_{max}$ in $mm\,s^{-1}$ with $m$ in kg and $d$ in metres. For $m = 100\,kg$ (see above), equation (15) thus predicts, for example, $v_{max}$ $c.$ $100\,mm\,s^{-1}$ at $d = 100\,m$ and $v_{max}$ $c.$ $2\,mm\,s^{-1}$ at $d = 1000\,m$. Conversely, BS7385-2 is primarily concerned with specifying allowable levels of ground vibration to avoid damage to buildings. It recommends frequency-dependent allowable limits for components of peak ground velocity ranging linearly from $15\,mm\,s^{-1}$ at 4 Hz to $20\,mm\,s^{-1}$ at 15 Hz and $50\,mm\,s^{-1}$ at 40 Hz to avoid cosmetic damage. As an alternative, BS6472-2 recommended that PGV in the seismic wavefield incident on any residential building should not exceed $10\,mm\,s^{-1}$ during the working day (8 a.m. to 6 p.m. on Mondays to Fridays or 8 a.m. to 1 p.m. on Saturdays), $2\,mm\,s^{-1}$ at night (11 p.m. to 7 a.m.), or $4.5\,mm\,s^{-1}$ at other times, these guidelines being for avoidance of disturbance to occupants rather than considerations of damage. An alternative lower limit of $6\,mm\,s^{-1}$ during the working day was also recommended, with PGV between 6 and $10\,mm\,s^{-1}$ allowable if justifiable on a case-by-case basis. For comparison, in the USA Siskind et al. (1980) recommended that PGV $\leq 12.7\,mm\,s^{-1}$ (i.e. $\leq 0.5\,inches\,s^{-1}$) is 'safe' (i.e. will not cause even cosmetic damage), but occupants of buildings might nevertheless experience nuisance from less strong ground vibrations. The BS6472-2 guideline would prevent, for example, a quarry operator from blasting during the working day using 100 kg explosive charges if there is a residential property within $c.$ 530 m and would limit blasting outside the working day to charges of <53 kg and at night to charges of <27 kg if the nearest residential property were at this distance threshold.

Figure 1 compares the UK regulatory guidelines for PGV from quarry blasting and other thresholds of PGV estimated to cause hazards (i.e. damage) or various forms of environmental nuisance with the predictions of PGV as a function of magnitude that have been discussed above. It is thus apparent, notwithstanding the tendency of our spectral technique to over-predict PGV, that for 'fracking' at 2.5 km depth, resulting in tensile fracture earthquakes with $B = 1.4$, the suggestion by De Pater & Baisch (2011) of a limit to induced microseismicity of $M_L$ 1.7 is roughly equivalent to the BS6472-2 guideline that exposure to PGV from quarry blasting at night should not exceed $2\,mm\,s^{-1}$. This threshold also roughly matches the limit to PGV expected from movement of heavy vehicles past residential property (from NCHRP 1999), as might be expected, for example, to deliver supplies to any shale gas project. Likewise, the BS6472-2 upper limit to exposure to PGV from quarry blasting during the working day of $10\,mm\,s^{-1}$ roughly matches the upper bound to PGV expected for a microearthquake of $M_L$ 3 at 2.5 km depth. Conversely, and again notwithstanding the tendency of our spectral technique to over-predict PGV, the threshold of $M_L$ 0.5 suggested by Green et al. (2012) and adopted by DECC (2013b) for suspension of 'fracking' would correspond to very small values of PGV (e.g. $c.$ $0.5\,mm\,s^{-1}$ for tensile fracture earthquakes with $B = 1.4$; Figure 1; which would reduce to

$c.$ $0.4\,mm\,s^{-1}$ if the radiation pattern for vertical tensile fractures were taken into account; see the Appendix). This seems excessively cautious and, thus, inappropriate as a regulatory limit; ground vibration at this level would have a chance of being felt only under low ambient noise conditions and would be exceeded by the effects of many domestic activities. Likewise, the suggestion by Bull (2013) that 'fracking' should be suspended following the occurrence of any induced earthquake of $M_L \geq 4.5$ is based on the notion that this threshold corresponds to PGV $c.$ $34\,mm\,s^{-1}$ and epicentral intensity V (see Wald et al. 1999). However, it is much too high as a threshold for regulating ground vibrations on the basis that they result in environmental nuisance comparable with other potential causes; it is a threshold for the prediction of damage to buildings. On the other hand, the statement by Mair et al. (2012, p. 16) that 'vibrations from a seismic event of magnitude $2.5\,M_L$ are broadly equivalent to the general traffic, industrial and other noise experienced daily' is not entirely correct. From Figure 1, an $M_L$ 2.5 tensile fracture earthquake with $B = 1.4$ at 2.5 km depth would be expected to produce a PGV of $c.$ $6\,mm\,s^{-1}$, albeit reducing to $c.$ $4\,mm\,s^{-1}$ if the radiation pattern were taken into account. This is rather greater than might be expected for traffic (for example, at a distance of $c.$ 8 m from a moving lorry the PGV would be $c.$ $2\,mm\,s^{-1}$ according to NCHRP (1999)) although it would be within the $10\,mm\,s^{-1}$ regulatory limit for quarry blasting during the working day.

We thus suggest that the existing UK regulatory thresholds for ground vibrations induced by quarry blasting can form the basis of regulatory limits for 'fracking': a PGV of $10\,mm\,s^{-1}$ during the working day, $2\,mm\,s^{-1}$ at night, and $4.5\,mm\,s^{-1}$ at other times. These thresholds might be considered reasonable limits on the levels of ground vibration that can be anticipated in any area when 'fracking' is under way, and might also be used as criteria for the suspension of fracking to avoid the possibility of a larger event occurring that might exceed these PGV values. As noted above, for tensile fracture earthquakes caused by 'fracking' at a depth of 2.5 km these 'working day' and 'night time' thresholds correspond roughly to magnitudes of 3.0 and 1.7. Figure 2 illustrates how the associated magnitude thresholds scale for 'fracking' at different depths, to maintain the same limits for PGV at the Earth's surface in the epicentral area, subject to the adoption of the scaling behaviour for the induced seismicity that is discussed above, for both tensile fracture and shear fracture earthquakes. Furthermore, it is apparent that, although such events will be very rare (see Fisher & Warpinski 2012), the largest possible tensile fracture earthquakes that might occur are capable of producing PGV well in excess of the $10\,mm\,s^{-1}$ regulatory limit that we have suggested, if consistency with existing regulations for quarrying is to be achieved. The possibility of such large PGV values arising from 'fracking' cannot be excluded, but the probability of such long fractures developing in a single rupture is evidently very low (see Davies et al. 2013), so any resulting nuisance could be covered by a system of compensation. The long-standing systems that operate in the UK, whereby, for example, the Coal Authority compensates owners of property for damage caused by mining subsidence (e.g. Coal Authority 2004) or the Royal Air Force provides compensation for damage caused by sonic booms from military aircraft, provide robust precedents.

It is apparent that the development of any 'fracking' site should be preceded by site surveys (e.g. using 3D seismic reflection profiling) to exclude the presence of any pre-existing faults large enough that, if they were to slip in an induced earthquake, would result in ground motions on a scale that could cause damage. Modern seismic survey techniques can readily resolve faults with dimensions of tens of metres and vertical offsets of $c.$ 10 m (e.g. Arthur et al. 2013), provided the interpretation is carried out with appropriate expertise (see Bond et al. 2012). Thought also needs to be given to the permeability of such faults, as this influences the potential for 'fracking' fluid to escape into them and potentially lubricate larger patches of fault (see Lunn et al. 2008; Solum et al. 2010). A trade-off evidently
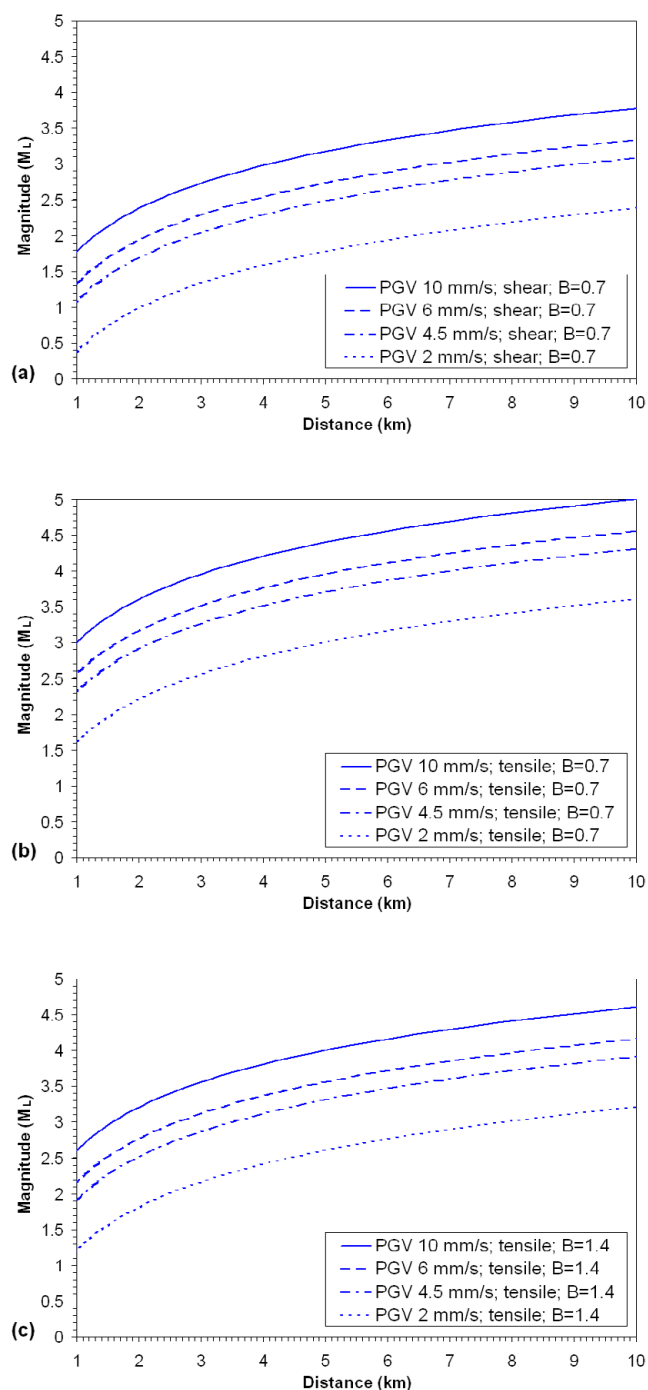
**Fig. 2.** Predictions of magnitude thresholds for a given PGV at a given epicentral distance from an earthquake source of a given magnitude, calculated, using the same procedures and parameter values as for Figure 1, for the limits for PGV at different times of day that are recommended by BS6472-2. **(a)** Shear fracture earthquakes with $B = 0.7$; **(b)** tensile fracture earthquakes with $B = 0.7$; **(c)** tensile fracture earthquakes with $B = 1.4$.

exists between the level of detail to which such surveys are undertaken and the consequences of induced nuisance shear earthquakes on faults that are overlooked. The graphs in Figures 1 and 2 can thus help guide such decision-making, as well as informing consideration of pressure and volume of 'fracking' fluid to limit the size of 'worst case scenario' induced tensile earthquakes, rare though the latter might be. Pending further refinements (such as consideration of random phase variations between different frequency components of the seismic waves and consideration of the spectral content of the seis-

mic radiation in relation to human perceptions of nuisance), the recommendations summarized in Figure 2 can thus provide a basis for regulation of induced seismicity from 'fracking'. To implement them will require any site at which 'fracking' is undertaken to be instrumented with seismographs for real-time monitoring of the activities, as specified by Mair *et al.* (2012) (cf. Warpinski 2013). Such installations will require three-component broadband seismometers of appropriate bandwidth to allow spectral studies to determine seismic moment and to permit reliable identification of seismic phases for earthquake location. Once determined, the seismic moment can be converted to $M_w$ using equation (2) and the combination of source depth, magnitude and focal mechanism compared with the recommendations in Figure 2 to determine the chance of any 'nuisance'-level ground vibrations occurring anywhere at the Earth's surface and, thus, whether any action need be taken, such as to modify the 'fracking' process or compensate anyone affected. The requirement for such monitoring measures should not impose any onerous burden on the developer of any proposed shale gas site. Moreover, the ability to seismically monitor the manner in which induced microearthquakes propagate over time away from sites of fluid injection will provide useful information to developer; for example, it allows the permeability of the rock mass to be determined using standard techniques (e.g. Li 1984), and provides a means of maintaining the propagation of fractures at a safe distance from any rock unit that should not be fractured, say because it forms an aquifer (cf. Davies *et al.* 2012; Fisher & Warpinski 2012; Geiser *et al.* 2012). Propagation of fractures into an aquifer is unlikely to result in aquifer pollution, given the lack of any sustained hydraulic gradient towards the Earth's surface from a naturally under-pressured shale gas zone (Younger 2014). Rather, avoidance of 'fracking' connections into aquifers is first and foremost a concern for the developer, as interception of permeable, water-bearing zones in sterile overburden is highly likely to flood-out the underlying gas-producing zones just developed at great expense. For this reason, microseismic monitoring of 'fracking' processes is routine (e.g. Warpinski 2013): the amount of 'force' applied in fracking indeed tends to be strictly controlled, so it is limited to that required to increase the permeability of the target gas-rich zones, avoiding sterile overburden, especially where this may be water-bearing. The same microseismic data could also be readily used to assess compliance with any framework for regulating induced seismicity. Furthermore, the eventual recording of large quantities of data of this type should be beneficial to future refinements of any regulatory framework for the induced ground vibrations and may contribute to refining theory for the triggering and scaling behaviour of microearthquakes.

Nonetheless, as discussed, for example, by Mair *et al.* (2012), a proportion of the fluid injected to 'frack' a borehole returns to the surface when the well is subsequently depressurized; although this 'flowback fluid' can be recycled, ultimately, any shale gas production development must be accompanied by a wastewater disposal system. In the USA it is common practice to dispose of wastewater from this and other industrial processes in boreholes. This action (rather than 'fracking' *per se*) appears to be the main cause of the significant increase in seismicity observed in the USA over the past decade (e.g. Ellsworth 2013; Hitzman *et al.* 2013; Van Der Elst *et al.* 2013). Furthermore, as already noted, much larger induced earthquakes are attributed to this mechanism than to the 'fracking' directly, such as the aforementioned Prague, Oklahoma, event. The case study of the Denver, Colorado, sequence of induced earthquakes in 1967–1968 (including the $M_w$ 4.8 event of 9 August 1967), following disposal in a deep borehole of hazardous wastewater from the manufacture of nuclear weapons, is indeed well known (e.g. Healy *et al.* 1968; Herrmann *et al.* 1981; Hsieh & Bredehoeft 1981; Ellsworth 2013). Mair *et al.* (2012) described the extant regulatory framework for wastewater disposal in the UK; DECC (2014) has subsequently established a regulatory framework specifically for the disposal of 'flowback fluid'. This latter

document lists the procedures that will be allowable; however, disposal down boreholes is not given as an option, because it is forbidden under the terms of the European Water Framework Directive and its daughter Groundwater Directives. Reinjection of spent 'fracking' fluids will therefore not be permitted in the UK: hence, the issue of induced seismicity caused by borehole disposal of 'flowback fluid' will simply never arise in this jurisdiction.

## Conclusions

In December 2013 the UK authorities issued a formal set of regulations governing 'fracking', which include the threshold of $M_L$ 0.5 for the suspension of operations (DECC 2013b). Fortunately, this document also states that this set of regulations will be 'subject to review'; it is our hope that the contents of the present paper may be of value in guiding these authorities towards an improved regulatory process, to avoid unfairly disadvantaging the new shale gas industry relative to existing industries (many of which are far more carbon-intensive: for instance, opencast coal mining, which is subject to the quarrying regulations discussed above). We indeed propose a framework for regulating induced microseismicity from 'fracking' in the UK based on the existing regulatory limits applicable to quarry blasting (from BS6472-2); namely, that peak ground velocities in the seismic wavefield incident on any residential property should not exceed $10\,\mathrm{mm\,s^{-1}}$ during the working day, $2\,\mathrm{mm\,s^{-1}}$ at night, or $4.5\,\mathrm{mm\,s^{-1}}$ at other times. Levels of vibration of this order do not constitute a hazard, but are similar in magnitude to the 'nuisance' vibrations that result from activities such as slamming doors, walking on a wooden floor or driving a heavy goods vehicle down a residential road (Fig. 1). Using a simple technique based on analysis of the spectra of seismic S-waves, we have shown that this proposed daytime regulatory limit for PGV is likely to be satisfied directly above the source of a magnitude 3 induced earthquake at a depth of 2.5 km (Fig. 1), and illustrate how the proposed regulatory limits scale in terms of magnitudes of induced earthquakes at other distances (Fig. 2). Previous experience (cf. Davies *et al.* 2012, 2013; Fisher & Warpinski 2012) indicates that the length of the fracture networks that are produced by 'fracking' cannot exceed *c.* 600 m, this limit being determined by the available volume and pressure of the 'fracking' fluid. The development of a fracture network of this size in one single tensile rupture would correspond to an induced earthquake *c.* magnitude 3.6, although the probability of this happening is very low. Events of this size would result in PGV above our proposed maximum regulatory limit (Figs 1 and 2) and might be sufficient to cause minor damage to property, such as cracked plaster; however, such occurrences, if they ever occur, will be infrequent. If any such incidents do occur, they could be readily handled under a system of compensation similar to that operated by the Coal Authority for mining subsidence, or that operated by the Royal Air Force to compensate for the effects of sonic booms. The data to operate such a system will be available, as seismic monitoring of 'fracking' is essential both to follow the progression of the process in the interests of the developer, and also to demonstrate compliance with any regulatory framework. There is thus no scientific reason why seismicity induced by shale gas 'fracking' should not be regulated in a manner analogous to the way in which quarry blasting has been successfully and uncontroversially regulated in the UK for decades.

## Appendix: Seismic radiation from tensile fractures; comparison with shear fractures

Other workers have previously derived from first principles or utilized the seismic radiation patterns for P- and S-waves radiated by tensile fractures (e.g. Rice 1980; Walter & Brune 1993; Shi & Ben-Zion 2009; Eaton *et al.* 2014). These analyses are based on the more general literature in fracture mechanics (e.g. Griffith 1924; Sneddon 1951; Eshelby 1957), which itself builds on earlier analyses (e.g. Rankine 1843, 1858). However, the practical implications of such results for regulating 'fracking' have not previously been assessed. Furthermore, most previous treatments have expressed the theoretical results in terms of an idealized rock rheology with a Poisson's ratio of 0.25, rather than stating them in general terms that are applicable to any linear elastic rheology.

The relevant theory for tensile fracture earthquakes is based on considerations of energy storage by elastic deformation during the opening of a tensile crack, from Sneddon (1951). This theory thus concerns mechanical properties of rocks, which include shear modulus ($\mu$), Young's modulus ($E$), density ($\rho$), P-wave and S-wave velocities ($v_P$ and $v_S$) and acoustic impedances ($Z_p$ and $Z_s$), Poisson's ratio ($v$), and the first Lamé parameter ($\lambda$), which are interrelated using standard formulae such as

$$v_s \equiv \sqrt{\frac{\mu}{\rho}} \tag{A1}$$

$$v_P \equiv \sqrt{\frac{\lambda + 2\mu}{\rho}} \equiv \sqrt{\frac{2\mu(1-v)}{\rho(1-2v)}} \equiv v_s\sqrt{\frac{2(1-v)}{(1-2v)}} \equiv bv_s \tag{A2}$$

$$E \equiv 2(1+v)\mu \tag{A3}$$

$$v \equiv \frac{(v_P/v_s)^2 - 2}{2(v_P/v_s)^2 - 2} \tag{A4}$$

$$Z_s \equiv \rho\,v_s \tag{A5}$$

and

$$\lambda \equiv \frac{2\mu v}{1-2v}. \tag{A6}$$

Much of the relevant analysis for the properties of seismic radiation from tensile fractures was worked out by Walter & Brune (1993); however, their analysis was subject to the simplifying assumption that $v = 0.25$, which, for example, constrains $\lambda = \mu$ and $v_P = \sqrt{3}\,v_s$. Because we are now concerned with tensile fractures in lithologies for which $v \neq 0.25$, we shall derive some of the relevant equations over again, without building in this simplifying assumption.

Sneddon (1951; equation 128 on p. 490) showed that a circular crack of radius $a$, which opens in rock as a result of a uniform excess internal pressure $P$, has an elliptical profile with each face displaced by a distance $w$ where

$$w(r) = \frac{4P(1-v^2)}{\pi E}\sqrt{(a^2 - r^2)} \tag{A7}$$

$r$ being the distance from the centre of the crack. Sneddon (1951; equation 131 on p. 491) also showed by integration that the elastic strain energy $W$ required to open this crack is

$$W = \frac{8P^2a^3\left(1-\nu^2\right)}{3E} = \frac{4P^2a^3\left(1-\nu\right)}{3\mu}. \tag{A8}$$

Walter & Brune (1993) stated this expression as

$$\lambda = \frac{P^2a^3}{\mu} \tag{A9}$$

which is consistent for $\nu = 0.25$.

Equating $u = 2w$ and using equation (1), the seismic moment of the tensile fracture earthquake that occurs if the crack described in equation (A7) forms in a single rupture can be determined as

$$M_o = \int_0^a \frac{8\mu P\left(1-\nu^2\right)}{\pi E}\sqrt{\left(a^2 - r^2\right)} \times 2\pi r\,\mathrm{d}r \tag{A10}$$

or, given the interrelationships noted above between $E$, $\mu$ and $\nu$,

$$M_o = \frac{8}{3}P\left(1-\nu\right)a^3. \tag{A11}$$

For $\nu = 0.25$, equation (A11) simplifies to the form $M_o = 2Pa^3$ stated by Eaton *et al.* (2014), although this limit to validity was not noted by those researchers.

Theory for the spectral amplitudes of the displacement in seismic waves from conventional earthquakes (e.g. Aki 1967; Brune 1970) was extended by Walter & Brune (1993) to tensile fracture earthquakes, with some aspects generalized for $\lambda \neq \mu$ or $\nu \neq 0.25$ by Shi & Ben-Zion (2009). Spectra of tensile fracture earthquakes are thus flat at frequencies $f$ below the corner frequency $f_c^T$, at low-frequency asymptotes $\Omega^{TP}$ and $\Omega^{TS}$ given by

$$\Omega^{TP} = \frac{R_{\theta\varphi}{}^{TP}M_o}{4\pi\rho v_P{}^3R} = \frac{\left[\lambda/\mu + 2\cos^2\left(\theta\right)\right]M_o}{4\pi\rho v_P{}^3R} \tag{A12}$$

and

$$\Omega^{TS} = \frac{R_{\theta\varphi}{}^{TS}M_o}{4\pi\rho v_S{}^3R} = \frac{\sin\left(2\theta\right)M_o}{4\pi\rho v_S{}^3R} \tag{A13}$$

where $R_{\theta\varphi}{}^{TP}$ and $R_{\theta\varphi}{}^{TS}$ are the directional coefficients for the P- and S-wave radiation patterns from a tensile source, $R$ is distance from the source, and the angle $\theta$ is measured from zero in the direction perpendicular to the fracture plane. The angular variations in $R_{\theta\varphi}{}^{TP}$ and $R_{\theta\varphi}{}^{TS}$ have been depicted graphically in multiple publications (e.g. as fig. 2 of Walter & Brune (1993), fig. 2b of Shi & Ben-Zion (2009), fig. 2 of Vavryčuk (2011), and fig. 2 of Eaton *et al.* (2014)).

The analysis by Walter & Brune (1993) to determine the corner frequencies for the P- and S-waves radiated by tensile fracture earthquakes, $f_c^{TP}$ and $f_c^{TS}$ (where $\zeta_T = f_c^{TP}/f_c^{TS}$), also requires generalization for $\lambda \neq \mu$. This analysis equates the integrals of the energy radiated as P- and S-waves at all frequencies up to $f_c^{TP}$ and $f_c^{TS}$, averaged over all directions around the seismic source, to a fraction $\eta$ of the elastic strain energy available, from equation (A8). This in turn requires the angular averages of the squares of the trigonometric functions that appear in the numerators of equations (A12) and (A13). For equation
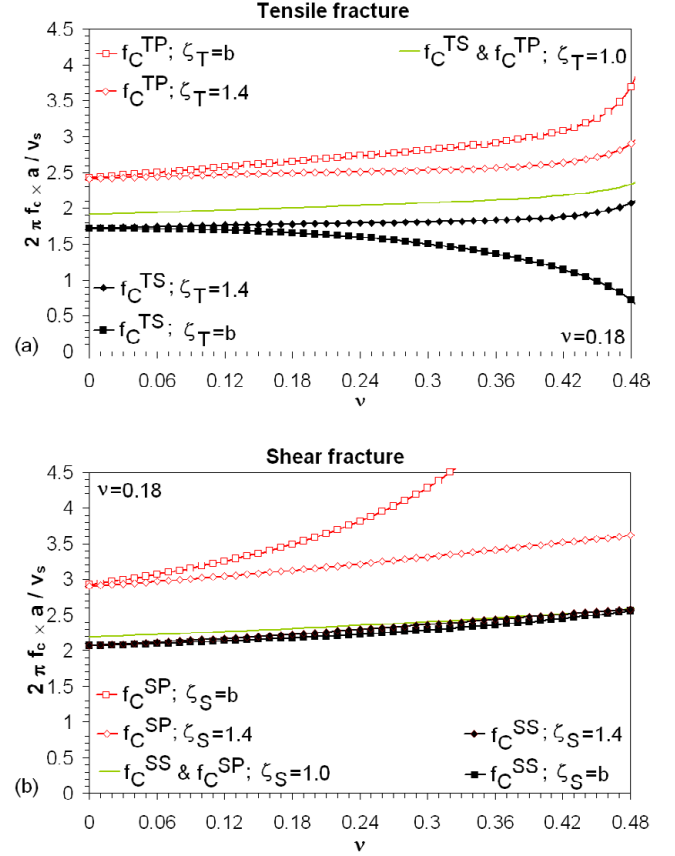


**Fig. A1.** (**a**) Graphs illustrating the variations with $\nu$ of P-wave and S-wave corner frequencies for tensile earthquakes, plotted as $f_c^{TP} \times 2\pi a/v_s$ and $f_c^{TS} \times 2\pi a/v_s$, for different values of $\zeta_T$, calculated as explained in the text. (**b**) Equivalent graphs illustrating the variations in P-wave and S-wave corner frequencies for shear earthquakes, plotted as $f_c^{SP} \times 2\pi a/v_s$ and $f_c^{SS} \times 2\pi a/v_s$, for different values of $\zeta_S$. The graphs for $\zeta_T$ or $\zeta_S = b$ and $\zeta_T$ or $\zeta_S = 1.4$ converge as $\nu \to 0$ because $b \to 1.4$ as $\nu \to 0$, $b$ being $\sqrt{2}$ or $c$. 1.41 when $\nu = 0$.

(A13) this term was determined as 8/15 by Walter & Brune (1993); that for equation (A12) requires evaluation, for $\lambda \neq \mu$, as $k/15$, where

$$k = \frac{15}{2}\int_0^\pi \left[c + \cos^2\left(\theta\right)\right]^2\sin\left(\theta\right)\mathrm{d}\theta = 15c^2 + 20c + 12 \tag{A14}$$

with $c = \lambda/\mu$. Thus, $k = 47$ when $c = 1$, consistent with the Walter & Brune (1993) analysis.
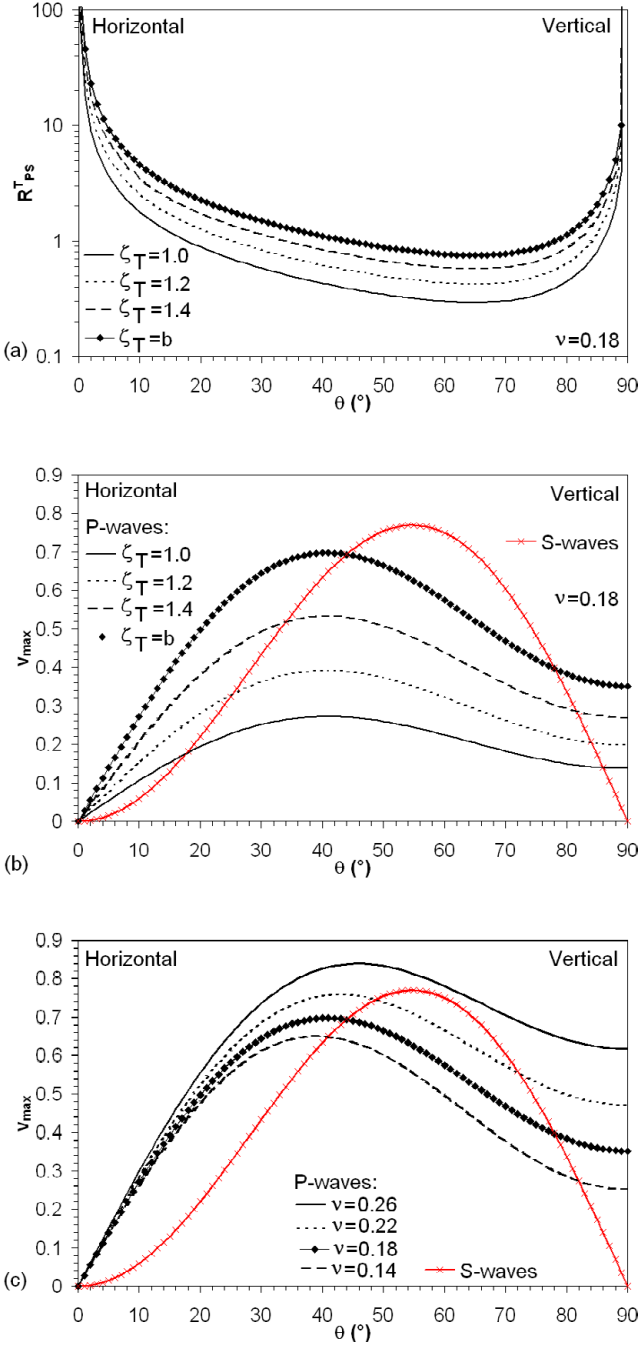
Putting all this together gives

$$f_c^{TS} = \left[\frac{45\pi b^5\eta}{\left(1-\nu\right)\left(k\zeta_T{}^3 + 8b^5\right)}\right]^{1/3}\frac{v_S}{2\pi a} \tag{A15}$$

which, for $b = \sqrt{3}$, $\nu = 0.25$, and $k = 47$, is consistent with equation (17) of Walter & Brune (1993). Equation (A15) can also be written as

$$f_c^{TS} = \Lambda_T \frac{v_S}{2\pi a} \tag{A16}$$

where

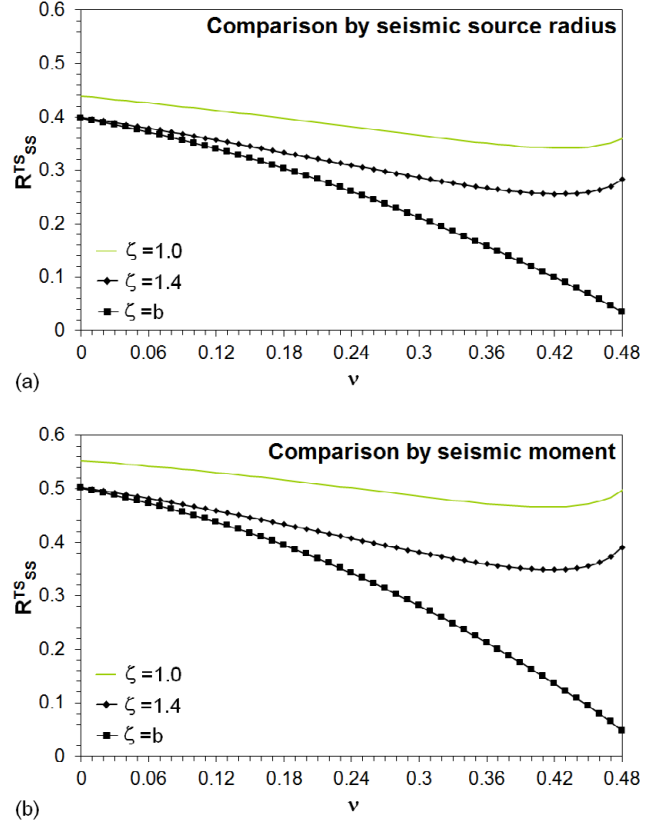$$\Lambda_T = \left[\frac{45\pi b^5\eta}{\left(1-\nu\right)\left(k\zeta_T{}^3 + 8b^5\right)}\right]^{1/3}. \tag{A17}$$

(a)

(b)

(c)

**Fig. A2.** Effects of raypath inclination, $\theta$, on predictions of peak ground velocity for tensile earthquakes on vertical fractures. **(a)** Graph of $R^T_{PS} \equiv v_{max}^{TP}/v_{max}^{TS}$ for $v = 0.18$ (for which $b \approx 1.60$ and $\lambda/\mu = 0.5625$), using equations (A57) and (A58), for the specified values of $\zeta_T$. **(b)** Graphs of $v_{max}^{TP}$ and $v_{max}^{TS}$ in relative units (for $C/z = 1$), using equations (A57) and (A58) again with $v = 0.18$, for different values of $\zeta_T$. **(c)** Graphs of $v_{max}^{TP}$ and $v_{max}^{TS}$, likewise in relative units and based on equations (A57) and (A58), for $\zeta_T = b$ and different values of $v$.

Using equation (A11), equation (A15) can also be expressed in terms of $M_o$ rather than $a$, as

$$f_c^{TS} = \left[\frac{8(1-v)P}{3M_o}\right]^{1/3} \Lambda_T \frac{v_S}{2\pi} = \left[\frac{120\pi b^5 \eta P}{M_o\left(k\zeta_T^3 + 8b^5\right)}\right]^{1/3} \frac{v_S}{2\pi} \quad (A18)$$



(a)

(b)

**Fig. A3.** Graphs of $R_{TS}^{SS}$ as a function of $v$ and $\zeta$ for the case where $P/S = 0.5$ **(a)** Comparison of tensile and shear earthquakes with the same source radius, based on equation (A64). **(b)** Comparison of tensile and shear earthquakes with the same seismic moment, based on equation (A65).

The parameter $\Lambda_T$ thus factors in both the direct dependence of corner frequencies on $v$ and the indirect dependence owing to $b$ and $k$ also depending on $v$ (equations (A2), (A6) and (A14)). The resulting variations of $\Lambda_T$ with $v$, illustrated for $\eta = 0.5$ (Fig. A1a), are consistent with values determined previously for $v = 0.25$ by Walter & Brune (1993): with $\zeta_T = 1.0$, $2\pi f_c^{TP} = 2\pi f_c^{TS} \approx 2.05 v_S/a$; with $\zeta_T = 1.4$, $2\pi f_c^{TP} \approx 2.51 v_S/a$ and $2\pi f_c^{TS} \approx 1.80 v_S/a$; and with $\zeta_T = \sqrt{3}$, $2\pi f_c^{TP} \approx 2.75 v_S/a$ and $2\pi f_c^{TS} \approx 1.59 v_S/a$.

However, although it has been generalized to any value of $v$, the above analysis incorporates the assumption of uniform $P$, and so neglects the vertical pressure gradient in the 'fracking' fluid that is causing a crack to open; it is thus valid for vertical fractures only if $P \gg 2\rho_f g a$ (where $\rho_f$ is the density of the 'fracking' fluid and $g$ is the acceleration due to gravity) or $a \ll P/(2\rho_f g)$, so if $P = 1\,\text{MPa}$ and $\rho_f = 1000\,\text{kg m}^{-3}$ this analysis is valid only if $a \ll 50\,\text{m}$, or $M_o < c.\,3 \times 10^{11}\,\text{N m}$ (equation (A11)), or $M_W < c.\,1.6$ (equation (3)).

The corresponding analysis for a shear fracture, also provided by Walter & Brune (1993) only for $\lambda = \mu$, can likewise be generalized for $\lambda \neq \mu$ by a very similar procedure starting from equations (5.3), (5.6) and (5.7) of Eshelby (1957). One thus obtains, for a narrow circular shear fracture of radius $a$ with elliptical cross-section, which forms as a result of a shear stress $S$, that the shear displacement across the fracture, $u$, is

$$u(r) = \frac{8S\,(1-v)}{\pi\mu\,(2-v)}\sqrt{\left(a^2 - r^2\right)}. \quad (A19)$$

Thus, from equation (1),

$$M_o = \int_0^a \frac{8S(1-\nu)}{\pi(2-\nu)} \sqrt{(a^2 - r^2)} \times 2\pi r \, dr = \frac{16S(1-\nu)a^3}{3(2-\nu)} \quad (A20)$$

which simplifies, for $\nu = 0.25$, to the standard formula $M_o = (16/7)a^3\Delta\sigma$ (e.g. Lay & Wallace 1995) if the stress drop $\Delta\sigma$ is equated to $S$. The work done creating this fracture is $W_S$, where

$$W_S = \frac{8S^2a^3(1-\nu)}{3\mu(2-\nu)} = \frac{\pi^2 \mu a \varepsilon^2 (2-\nu)}{24(1-\nu)} \quad (A21)$$

with $\varepsilon$ denoting the maximum shear displacement (at $r = 0$), and the low-frequency asymptotes of the source spectrum are

$$\Omega^{SP} = \frac{R_{\theta\varphi}{}^{SP}M_o}{4\pi\rho v_P{}^3 R} = \frac{\sin(2\theta)\cos(\phi)M_o}{4\pi\rho v_P{}^3 R} \quad (A22)$$

and

$$\Omega^{SS} = \frac{R_{\theta\varphi}{}^{SS}M_o}{4\pi\rho v_s{}^3 R} = \frac{|\cos(2\theta)\cos(\phi)\boldsymbol{\theta} - \cos(\theta)\sin(\phi)\boldsymbol{\phi}| M_o}{4\pi\rho v_S{}^3 R} \quad (A23)$$

where $R_{\theta\varphi}{}^{SP}$ and $R_{\theta\varphi}{}^{SS}$ are analogous to $R_{\theta\varphi}{}^{TP}$ and $R_{\theta\varphi}{}^{TS}$ but for a shear source, $\varphi$ is azimuth, measured relative to the slip vector, $f_c^{SP}$ and $f_c^{SS}$ are corner frequencies for the P- and S-waves radiated by shear fracture earthquakes (with $\zeta_S = f_c^{SP}/f_c^{SS}$), and $\boldsymbol{\theta}$ and $\boldsymbol{\phi}$ are unit vectors in mutually perpendicular directions transverse to the radial direction from the source, in the senses indicated in figure 1 of Shi & Ben-Zion (2009). With $\nu = 0.25$, these equations reduce to equations (21)–(24) of Walter & Brune (1993); in particular, equation (A20) reduces to the standard form given by equation (7), with the initial shear stress applied to the fracture, $S$ in equation (A20), equivalent to the coseismic stress drop $\Delta\sigma$ that appears in equation (7).

Similar analysis to that for the tensile fracture, utilizing the angular averages of the squares of $R_{\theta\varphi}{}^{SP}$ and $R_{\theta\varphi}{}^{SS}$, determined as 4/15 and 2/5 (e.g. Aki & Richards 1980, p. 120), gives

$$f_c^{SS} = \left[ \frac{45\pi(2-\nu)b^5\eta}{(1-\nu)(8\zeta_S{}^3 + 12b^5)} \right]^{1/3} \frac{v_S}{2\pi a} \quad (A24)$$

which, for $b = \sqrt{3}$ and $\nu = 0.25$, is consistent with equation (17) of Walter & Brune (1993). Equation (A15) can also be written as

$$f_c^{SS} = \Lambda_S \frac{v_S}{2\pi a} \quad (A25)$$

where

$$f_c^{SS} = \left[ \frac{45\pi(2-\nu)b^5\eta}{(1-\nu)(8\zeta_S{}^3 + 12b^5)} \right]^{1/3}. \quad (A26)$$

Using equation (A20), equation (A24) can also be expressed in terms of $M_o$ rather than $a$, as

$$f_c^{SS} = \left[ \frac{16(1-\nu)S}{3(2-\nu)M_o} \right]^{1/3} \Lambda_S \frac{v_S}{2\pi} = \left[ \frac{60\pi S b^5 \eta}{(2\zeta_S{}^3 + 3b^5)M_o} \right]^{1/3} \frac{v_S}{2\pi}. \quad (A27)$$

Like $\Lambda_T$, $\Lambda_S$ thus factors in both direct and indirect dependences of corner frequencies on $\nu$. The resulting variations of $\Lambda_S$ with $\nu$, illustrated for $\eta = 0.5$ (Fig. A1b), are consistent with the determination by Walter & Brune (1993) that with $\nu = 0.25$ and $\zeta_S = 1.4$, $2\pi f_c^{SS} \approx 2.31 v_S/a$.

As Walter & Brune (1993) showed, $\zeta$ must lie between unity and $b$. The upper limit of $\zeta = b$ is for a source that ruptures instantaneously, whereas the lower limit of $\zeta = 1$ is for a source for which the effective duration of rupture is long compared with the ratio of radius to seismic wave velocity, such that the observed corner frequency is determined entirely by the rupture time. Walter & Brune (1993) also considered an intermediate case where $\zeta = 1.4$; Eaton et al. (2014) also adopted this latter value of $\zeta$, although without noting this as the basis of their analysis. Many studies have noted that choice of rupture velocity (or choice of $\zeta$) has a substantial effect on amplitudes of seismic radiation; Figure A1 indicates that variations in $\nu$ can have comparable importance.

The case of a rectangular vertical fracture of height $H$ and length $L$, in the vertical and horizontal directions along the fracture plane, has been investigated by Fisher & Warpinski (2012) using theory by England & Green (1963) and Simonson et al. (1978). The width $w$ of such a fracture is thus taken as varying with the vertical coordinate $y$, measured upwards from the midpoint of the fracture (so $y$ ranges between $-H/2$ and $+H/2$), as

$$w(y) = \frac{(1-\nu)}{2\mu}(2P + Ky)\sqrt{(H^2 - 4y^2)} \quad (A28)$$

in rock of shear modulus $\mu$, where $P$ is the fluid pressure at depth $y = 0$ and

$$K = C - \rho g \quad (A29)$$

is the difference between the vertical stress gradient $C$ and the fluid pressure gradient $\rho g$, $\rho$ being the density of the fluid and $g$ the acceleration due to gravity. Horizontal variations in $w$ are neglected in this analysis, so the solution is two-dimensional. The minimum value of $P$, $P_{min}$, required to keep the fracture open, is

$$P_{min} = \frac{KH}{4} \quad (A30)$$

and the cross-sectional area $A$ of the fracture is

$$A = \frac{(1-\nu)\pi \, PH^2}{4\mu}. \quad (A31)$$

The volume of the fracture can thus be estimated as $V = AL$, so with $P$ set to the minimum value, from equation (A30), one obtains

$$V \approx \frac{(1-\nu)\pi KLH^3}{16\mu}. \quad (A32)$$

Fisher & Warpinski (2012) illustrated this calculation with an example, which we have converted into SI units, for $\mu = 11.5$ GPa and $\nu = 0.2$, in a region where $K = 6$ kPa m$^{-1}$ owing to the effect of $C = 16$ kPa m$^{-1}$, given that $\rho = 1000$ kg m$^{-3}$. A pressure $P = 0.9$ MPa could create a fracture with $H = 600$ m, which would have $w$ up to c. 5 cm, and with $L = 300$ m would require c. 5600 m$^3$ of fluid. However, to create a fracture with $H = 1200$ m would require $P = 1.8$ MPa and, even if $L$ remained only 300 m, c. 45000 m$^3$ of fluid. In practice, because fluid would leak into the surrounding rock mass rather than simply occupying the volume of such a large fracture, the volume that would need to be injected would be larger than these limiting values.

The seismic moment released if a fracture of height $H$ and length $L$ forms in a single rupture can be estimated by using $w$ from equation (A28) for $u$ in equation (1) and is

$$\mathrm{M_o} \approx \mu L \int_{-H/2}^{H/2} w \, dy \qquad (A33)$$

which evaluates, using equation (A30) as the condition for minimum pressure, as

$$\mathrm{M_o} \approx \frac{(1-\nu)\pi KLH^3}{16} = \frac{(1-\nu)\pi LH^2 P_{\min}}{4}. \qquad (A34)$$

The work done creating this fracture, $W$, is

$$W \approx L \int_{-H/2}^{H/2} w(y) \, p(y) \, dy \qquad (A35)$$

where $p$ is the pressure at vertical position $y$. At the minimum pressure condition for initiating a fracture of height $H$

$$p = K(y + H/2) \qquad (A36)$$

so $W$ can be evaluated, after many algebraic steps, as

$$W = \frac{5\pi (1-\nu) K^2 LH^4}{128\mu}. \qquad (A37)$$

Similar analysis to that discussed above for a circular tensile crack thus gives

$$f_c^{\mathrm{TS}} = \left[ \frac{2400 b^5 \eta}{(1-\nu)\left(k\zeta_T^3 + 8b^5\right)} \right]^{1/3} \frac{v_S}{2\pi \left(LH^2\right)^{1/3}} \qquad (A38)$$

or

$$f_c^{\mathrm{TS}} = \left[ \frac{150\pi KHb^5 \eta}{\mathrm{M_o}\left(k\zeta_T^3 + 8b^5\right)} \right]^{1/3} \frac{v_S}{2\pi}. \qquad (A39)$$

If $L = H = 2a$ then equation (A38) can be written, like equation (A15), in terms of $\Lambda_T$, with

$$\Lambda_T = \left[ \frac{300 b^5 \eta}{(1-\nu)\left(k\zeta_T^3 + 8b^5\right)} \right]^{1/3}. \qquad (A40)$$

Comparison of equations (A17) and (A40) indicates that for a given set of values of $a$, $b$, $k$, $\nu$, $\zeta_T$, and $\eta$, $\Lambda_T$ is greater by a factor of $[300/(45\pi)]^{1/3}$ or $c$. 1.3 for a square tensile fracture with a vertical pressure gradient than for a circular tensile fracture at constant pressure.

Stochastic modelling has not previously been applied to quantification of the hazard (or nuisance) caused by the microseismicity induced by 'fracking' in the UK. A formal analysis of this type will be reported elsewhere; in the mean time, a simpler approach will be provided here. Thus, if it is assumed that all frequency components radiated by the earthquake source in each type of seismic wave oscillate in phase (rather than having random phase relations) with spectral displacement amplitudes as described above (i.e. constant at $\Omega$ for $f \leq f_c$ and proportional to $f^{-2}$ for $f > f_c$, up to some limiting

frequency $mf_c$) and anelastic attenuation is neglected, the peak ground velocity $v_{\max}$ can be evaluated as

$$v_{\max} = 2\pi\Phi\Omega \left[ \int_0^{f_c} f \, df + \int_{f_c}^{mf_c} f_c^2 / f \, df \right] \qquad (A41)$$

or

$$v_{\max} = \pi\Phi\Omega f_c^2 (1 + 2B) \qquad (A42)$$

where $B = \ln(m)$. Here, $\Phi$ is the amplification coefficient of the seismic waves, caused by the Earth's free surface. In general, $\Phi$ varies with seismic wave type (P or S) and also varies in a complex manner with the inclination of seismic raypaths relative to the free surface (the full complexity of this variation is demonstrated, for example, in the equations listed by Aki & Richards (1980, p. 190)). Nonetheless, in some situations $\Phi$ has a simple form; notably, $\Phi = 2$ for vertically incident P-waves and SV-components of S-waves, as well as for SH-components of S-waves at all inclinations. The present analysis will thus proceed subject to the simplifying assumption that $\Phi = 2$ in all circumstances; however, appropriate terms for $\Phi$, $\Phi_P$ and $\Phi_S$ will be included in equations to facilitate future derivation of the more general case. Typical values of $\Phi$ for general raypath inclinations are smaller than this limiting value of $\Phi = 2$, so our simplifying assumption that $\Phi = 2$ is consistent with our general objective of making conservative predictions of $v_{\max}$. Another consequence of this simplifying assumption is that it avoids any dependence of predicted values of $v_{\max}$ on the azimuth of seismic raypaths relative to that of fault or fracture planes activated by 'fracking' and thus results in the ability to make predictions of $v_{\max}$ as functions of distance alone.

It follows, by combining equations (A20), (A22), (A23), (A27) and (A42), that for shear earthquakes on circular faults

$$v_{\max}^{\mathrm{SP}} = \frac{\Phi_P R_{\theta\varphi}^{\mathrm{SP}} \mathrm{M_o}^{1/3} b^{1/3} S^{2/3}}{16\pi^2 \rho v_S R} \left[ \frac{60\pi\eta}{\left(2\zeta_S^3 + 3b^5\right)} \right]^{2/3} \zeta_S^2 (1 + 2B) \qquad (A43)$$

or

$$v_{\max}^{\mathrm{SP}} = \frac{\Phi_P R_{\theta\varphi}^{\mathrm{SP}} ab^{1/3} S}{8\pi^2 \rho v_S R} \left[ \frac{60\pi\eta}{\left(2\zeta_S^3 + 3b^5\right)} \right]^{2/3} \left[ \frac{2(1-\nu)}{3(2-\nu)} \right]^{1/3} \zeta_S^2 (1 + 2B) \qquad (A44)$$

and

$$v_{\max}^{\mathrm{SS}} = \frac{\Phi_S R_{\theta\varphi}^{\mathrm{SS}} \mathrm{M_o}^{1/3} b^{10/3} S^{2/3}}{16\pi^2 \rho v_S R} \left[ \frac{60\pi\eta}{\left(2\zeta_S^3 + 3b^5\right)} \right]^{2/3} (1 + 2B) \qquad (A45)$$

or

$$v_{\max}^{\mathrm{SS}} = \frac{\Phi_S R_{\theta\varphi}^{\mathrm{SS}} ab^{10/3} S}{8\pi^2 \rho v_S R} \left[ \frac{60\pi\eta}{\left(2\zeta_S^3 + 3b^5\right)} \right]^{2/3} \left[ \frac{2(1-\nu)}{3(2-\nu)} \right]^{1/3} (1 + 2B). \qquad (A46)$$

In contrast, by combining equations (A11), (A12), (A13), (A18) and (A42), for tensile earthquakes on circular fractures under constant pressure

$$v_{max}^{TP} = \frac{\Phi_P R_{\theta\varphi}^{TP} M_o^{1/3} b^{1/3} P^{2/3}}{16\pi^2 \rho v_S R} \left[ \frac{120\pi\eta}{\left(k\zeta_T^3 + 8b^5\right)} \right]^{2/3} \zeta_T^2 \left(1 + 2B\right)$$

(A47)

or

$$v_{max}^{TP} = \frac{\Phi_P R_{\theta\varphi}^{TP} ab^{1/3} P}{8\pi^2 \rho v_S R} \left[ \frac{120\pi\eta}{\left(k\zeta_T^3 + 8b^5\right)} \right]^{2/3} \left[ \frac{(1-\nu)}{3} \right]^{1/3} \zeta_T^2 \left(1 + 2B\right)$$

(A48)

and

$$v_{max}^{TS} = \frac{\Phi_S R_{\theta\varphi}^{TS} M_o^{1/3} b^{10/3} P^{2/3}}{16\pi^2 \rho v_S R} \left[ \frac{120\pi\eta}{\left(k\zeta_T^3 + 8b^5\right)} \right]^{2/3} \left(1 + 2B\right)$$

(A49)

or

$$v_{max}^{TS} = \frac{\Phi_S R_{\theta\varphi}^{TS} ab^{10/3} P}{8\pi^2 \rho v_S R} \left[ \frac{120\pi\eta}{\left(k\zeta_T^3 + 8b^5\right)} \right]^{2/3} \left[ \frac{(1-\nu)}{3} \right]^{1/3} \left(1 + 2B\right).$$

(A50)

Furthermore, by combining equations (A12), (A13) (A34), (A39) and (A42), for tensile earthquakes on square vertical fractures (with $H=L$) under pressure that increases vertically,

$$v_{max}^{TP} = \frac{\Phi_P R_{\theta\varphi}^{TP} M_o^{1/3} b^{1/3} (KH)^{2/3}}{16\pi^2 \rho v_S R} \left[ \frac{150\pi\eta}{\left(k\zeta_T^3 + 8b^5\right)} \right]^{2/3} \zeta_T^2 \left(1 + 2B\right)$$

(A51)

or

$$v_{max}^{TP} = \frac{\Phi_P R_{\theta\varphi}^{TP} b^{1/3} KH^2}{32\pi^2 \rho v_S R} \left[ \frac{150\pi\eta}{\left(k\zeta_T^3 + 8b^5\right)} \right]^{2/3} \left[ \frac{\pi(1-\nu)}{2} \right]^{1/3} \zeta_T^2 \left(1 + 2B\right)$$

(A52)

and

$$v_{max}^{TS} = \frac{\Phi_S R_{\theta\varphi}^{TS} M_o^{1/3} b^{10/3} (KH)^{2/3}}{16\pi^2 \rho v_S R} \left[ \frac{150\pi\eta}{\left(k\zeta_T^3 + 8b^5\right)} \right]^{2/3} \left(1 + 2B\right)$$

(A53)

or

$$v_{max}^{TS} = \frac{\Phi_S R_{\theta\varphi}^{TS} b^{10/3} KH^2}{32\pi^2 \rho v_S R} \left[ \frac{150\pi\eta}{\left(k\zeta_T^3 + 8b^5\right)} \right]^{2/3} \left[ \frac{\pi(1-\nu)}{2} \right]^{1/3} \left(1 + 2B\right).$$

(A54)

We now investigate the variation in predicted maximum ground velocities for the P- and S-waves radiated by vertical tensile fractures with $\theta$, the angle between the raypath and the direction perpendicular to the fracture. This analysis considers the effect of the radiation patterns for P- and S-waves but excludes complications owing to scattering of waves or interconversions between wave types as a result of inhomogeneity in geological structure or the effect of the Earth's surface. Such effects are discussed in textbooks (e.g. Aki & Richards 1980, pp. 123–167) but have been kept outside the scope of the present study. In the vertical plane perpendicular to a fracture, $\theta$ is equivalent to the raypath inclination (i.e. $\theta=0°$ for horizontal raypaths and $\theta=90°$ for vertical raypaths). As already noted (equations (A12) and (A13)) these angular variations are determined by $R_{\theta\varphi}^{TP}$ and $R_{\theta\varphi}^{TS}$ where

$$R_{\theta\varphi}^{TP} = \lambda/\mu + 2\cos^2(\theta)$$

(A55)

and

$$R_{\theta\varphi}^{TS} = \sin(2\theta) = 2\sin(\theta)\cos(\theta).$$

(A56)

If the constant $C$ absorbs all the terms from equations (A48) and (A50) (or equations (A52) and (A54)) that are common for P- and S-waves, and the distance $R$ is written as $z/\sin(\theta)$, where $z$ is the depth of 'fracking', then, for a vertical tensile fracture,

$$v_{max}^{TP} = \frac{C\Phi_P}{z} \left[ \frac{\lambda}{\mu} + 2\cos^2(\theta) \right] \sin(\theta) \frac{\zeta_T^2}{b^3}$$

(A57)

and

$$v_{max}^{TS} = \frac{C\Phi_S}{z} \sin(2\theta)\sin(\theta).$$

(A58)

Figure A2a and b illustrate the variations in the ratio of $v_{max}^{TP}/v_{max}^{TS}$ and in $v_{max}^{TP}$ and $v_{max}^{TS}$ with $\theta$ for $\lambda/\mu=0.5625$, corresponding to $\nu=0.18$, and $\Phi_P=\Phi_S=2$, for different values of $\zeta_T$. Figure A2c shows the predictions of $v_{max}^{TP}$ and $v_{max}^{TS}$ for different values of $\nu$, in each case for $\zeta_T=b$. It is thus evident that for steep or subhorizontal raypaths $v_{max}^{TP} \geq v_{max}^{TS}$ but for raypaths oriented at strongly oblique angles to the vertical, $v_{max}^{TP} < v_{max}^{TS}$, unless $\nu$ is relatively large, in which case $v_{max}^{TP} \geq v_{max}^{TS}$ at all values of $\theta$.

These patterns can be investigated in more detail by differentiating equations (A57) and (A58):

$$\frac{\partial v_{max}^{TP}}{\partial \theta} = \frac{C\Phi_P \zeta_T^2}{zb^3} \left[ \frac{\lambda}{\mu} + 2\cos^2(\theta) - 4\sin^2(\theta) \right] \cos(\theta)$$

(A59)

and

$$\frac{\partial v_{max}^{TS}}{\partial \theta} = \frac{2C\Phi_S}{z} \sin(\theta) \left[ 2\cos^2(\theta) - \sin^2(\theta) \right].$$

(A60)

Solving equation (A59) with the derivative on its left-hand side set to zero demonstrates that $v_{max}^{TP}$ is at a minimum when $\cos(\theta)=0$, at $\theta=90°$ (see Fig. A2b), and at a maximum when $\lambda/\mu + 2\cos^2(\theta) = 4\sin^2(\theta)$ or

$$\cos^2(\theta) = \left[ \frac{2}{3} - \frac{\lambda}{6\mu} \right].$$

(A61)

R. WESTAWAY & P. L. YOUNGER

For $\nu = 0.18$ or $\lambda/\mu \approx 0.6$, values appropriate for Carboniferous mudstone (see the main text), this requires $\cos(\theta) \approx 0.75$ or $\theta \approx 41°$. However, for $\nu = 0.26$ or $\lambda/\mu \approx 1.0$ it would require $\cos(\theta) \approx 0.70$ or $\theta \approx 46°$; this shift in the value of $\theta$ marking the peak in $v_{max}^{TP}$ is evident in Figure A2c. Likewise, $v_{max}^{TS}$ is at a minimum (of zero) when $\sin(\theta) = 0$ or $\theta = 0°$ (see Fig. A2b), and at a maximum when $2\cos^2(\theta) - \sin^2(\theta) = 0$, or $\cos(\theta) = 1/\sqrt{3}$, at $\theta \approx 55°$, this maximum value (for $C/z = 1$, as plotted in Fig. A2b) being $\sin(110°) \times \sin(55°)$ or $c. 0.770$. The peak ground velocities thus occur for raypaths at angles to the vertical of $c. 44–49°$ for P-waves and $c. 35°$ for S-waves.

The threshold for $\nu$ at which the peak in $v_{max}^{TP}$ exceeds that for $v_{max}^{TS}$ can be determined by solving equations (A57) and (A58) simultaneously, with the former set for the value of $\cos(\theta)$ given by equation (A61)) and the latter set for $\cos(\theta) = 1/\sqrt{3}$. After numerous algebraic steps, one obtains for this threshold condition

$$\zeta_T^{\,2} = 2\sqrt{2} \,. \tag{A62}$$

For the limiting case where $\zeta_T = b$, this is equivalent to

$$\nu = \frac{\sqrt{2}-1}{2\sqrt{2}-1} \tag{A63}$$

or $\nu \approx 0.227$. This is consistent with Figure A2c, in which for $\nu = 0.22$ the peak of $v_{max}^{TP}$ is slightly smaller than that for $v_{max}^{TS}$.

The above discussion establishes that unless $\nu$ is relatively large, $v_{max}^{TS} > v_{max}^{TP}$. Similar analysis for shear earthquakes would likewise establish that $v_{max}^{SS} > v_{max}^{SP}$. To assess the applicability to tensile earthquakes of empirical prediction equations for ground motion from shear earthquakes, we thus determine the ratio $R_{TS}^{SS} \equiv v_{max}^{TS}/v_{max}^{SS}$. We set $\zeta_T = \zeta_S = \zeta$ and use in this comparison the angular averages of $R_{\theta\varphi}^{TS}$ and $R_{\theta\varphi}^{SS}$ which, as already noted, are $\sqrt{(8/15)}$ and $\sqrt{(2/5)}$, respectively. This comparison between tensile and shear earthquakes may be made either for events of equivalent source radius or of equivalent seismic moment. In the former case, combining equations (A46) and (A50) gives:

$$R_{TS}^{SS} = \sqrt{\left(\frac{4}{3}\right)} \left[\frac{\left(2\zeta_S^{\,3} + 3b^5\right)}{\left(k\zeta_T^{\,3} + 8b^5\right)}\right]^{2/3} \frac{P}{S} \left(4 - 2\nu\right)^{1/3}. \tag{A64}$$

Alternatively, comparison by seismic moment using equations (A45) and (A49) gives:

$$R_{TS}^{SS} = \frac{2^{5/3}}{\sqrt{3}} \left[\frac{\left(2\zeta_S^{\,3} + 3b^5\right)P}{\left(k\zeta_T^{\,3} + 8b^5\right)S}\right]^{2/3} \tag{A65}$$

Figure A3 illustrates the resulting variations in $R_{TS}^{SS}$ with $\nu$ and $\zeta$, for the case where $P = 0.5S$ (i.e. where the tensile strength is half of the cohesion). Predictions for the former case, using equation (A64), are illustrated in Fig. A3a. The resulting values of $R_{TS}^{SS}$ are always <0.45, and would thus not exceed 0.9, and so would always be <1, if $P = S$. In the latter case, using equation (A65), illustrated in Fig. A3b, values of $R_{TS}^{SS}$ are always <0.55; they would increase by a factor of $2^{2/3}$ or $c. 1.59$ if $P$ and $S$ were equal and so would, again, always be <1. Both sets of results are,

therefore, consistent with the deduction in the main text that a tensile fracture will result in lower amplitude ground vibrations than an equivalent shear fracture, whether the comparison is in terms of the radius or the seismic moment of the fracture.

## References

AGARWAL, K., MAYERHOFER, M.J. & WARPINSKI, N.R. 2012. Impact of geomechanics on microseismicity. In: SMITH, G. & STEWART, S. (eds) Proceedings of the Society of Petroleum Engineers/European Association of Geoscientists and Engineers European Unconventional Resources Conference and Exhibition, 20–22 March 2012, Vienna, Austria. Curran Associates, Red Hook, NY, 662–677.

AKI, K. 1967. Scaling law of seismic spectrums. Journal of Geophysical Research, 72, 1217–1231.

AKI, K. 1969. Analysis of the seismic coda of local earthquakes as scattered waves. Journal of Geophysical Research, 74, 615–631.

AKI, K. & CHOUET, B. 1975. Origin of coda waves: Source, attenuation and scattering effects. Journal of Geophysical Research, 80, 3322–3342.

AKI, K. & RICHARDS, P.G. 1980. Quantitative Seismology. Freeman, San Francisco, CA.

AKKAR, S. & BOMMER, J.J. 2007. Empirical prediction equations for peak ground velocity derived from strong-motion records from Europe and the Middle East. Bulletin of the Seismological Society of America, 97, 511–530.

ALLMANN, B.B. & SHEARER, P.M. 2009. Global variations of stress drop for moderate to large earthquakes. Journal of Geophysical Research, 114, B01310, http://dx.doi.org/10.1029/2009JB005821.

ANDREWS, I.J. 2013. The Carboniferous Bowland Shale gas study: geology and resource estimation. British Geological Survey for Department of Energy and Climate Change, London. https://www.gov.uk/government/uploads/system/uploads/attachment_data/file/226874/BGS_DECC_BowlandShaleGasReport_MAIN_REPORT.pdf (accessed 3 January 2014).

ARCHULETA, R.J., COTTON, F., CAUSSE, M. & CREMPIEN, J. 2012. Stress drop variability. In: OTH, A., MAYEDA, K. & RIVERA, L. eds. Proceedings, European Center for Geodynamics and Seismology Workshop 2012: Earthquake source physics on various scales. Luxembourg, 3–5 October 2012. ftp://ftp.ecgs.lu/public/publications/source2012/Presentations/Keynotes/ECGS2012_THU-02-Archuleta.pdf. (accessed 3 January 2014)

ARTHUR, J.M., LAWTON, D.C. & WONG, J. 2013. Physical seismic modeling of a near-vertical fault zone. In: GeoConvention 2013, Calgary, Canada, 6–10 May 2013, Abstracts Volume. Canadian Society of Petroleum Geologists, Calgary, AB. http://geoconvention.org/archives/2013abstracts/299_GC2013_Physical_seismic_modeling.pdf. (accessed 7 July 2014)

BARTOS, F.J. 2011. Siemens gas turbine breaks 60% efficiency barrier. http://www.plantengineering.com/industry-news/automation-news/single-article/siemens-gas-turbine-breaks-60-efficiency-barrier/42c56242c5c0ba803ab7fc5aa0d00336.html. (accessed 3 January 2014).

BCOGC 2012. Investigation of observed seismicity in the Horn River Basin. British Columbia Oil and Gas Commission, Fort St John, BC. http://www.bcogc.ca/node/8046/download?documentID=1270 (accessed 3 January 2014).

BGS 2011a. Blackpool earthquake, Magnitude 2.3, 1 April 2011. British Geological Survey, Keyworth. http://www.bgs.ac.uk/research/earthquakes/blackpoolApril2011.html (accessed 3 January 2014).

BGS 2011b. Blackpool earthquake, Magnitude 1.5, 27 May 2011. British Geological Survey, Keyworth. http://www.bgs.ac.uk/research/earthquakes/blackpoolMay2011.html (accessed 3 January 2014).

BISHOP, I., STYLES, P. & ALLEN, M. 1993. Mining-induced seismicity in the Nottinghamshire Coalfield. Quarterly Journal of Engineering Geology, 26, 253–279.

BOMMER, J.J. & ALARCÓN, J.E. 2006. The prediction and use of peak ground velocity. Journal of Earthquake Engineering, 10, 1–17.

BOMMER, J.J., STAFFORD, P.J., ALARCÓN, J.E. & AKKAR, S. 2007. The influence of magnitude range on empirical ground-motion prediction. Bulletin of the Seismological Society of America, 97, 2152–2170.

BOND, C.E., LUNN, R.J., SHIPTON, Z.K. & LUNN, A.D. 2012. What makes an expert effective at interpreting seismic images? Geology, 40, 75–78.

BOORE, D.M. 2003. Simulation of ground motion using the stochastic method. Pure and Applied Geophysics, 160, 635–676.

BOORE, D.M. & THOMPSON, E.M. 2012. Empirical improvements for estimating earthquake response spectra with random-vibration theory. Bulletin of the Seismological Society of America, 102, 761–772.

BOURNE, S.J. & WILLEMSE, E.J.M. 2001. Elastic stress control on the pattern of tensile fracturing around a small fault network at Nash Point, UK. Journal of Structural Geology, 23, 1753–1770.

BRAGATO, P.L. & SLEJKO, D. 2005. Empirical ground-motion attenuation relations for the Eastern Alps in magnitude range 2.5–6.3. Bulletin of the Seismological Society of America, 95, 252–276.

BRUNE, J.N. 1970. Tectonic stress and the spectra of seismic shear waves from earthquakes. *Journal of Geophysical Research*, **75**, 4997–5009.

BSI 1993. *Evaluation and measurement for vibration in buildings—Part 2: Guide to damage levels from groundborne vibration. BS 7385-2: 1993*. British Standards Institution, London.

BSI 2008. *Guide to evaluation of human exposure to vibration in buildings—Part 2: Blast-induced vibration. BS 6472-2: 2008*. British Standards Institution, London.

BULL, J. 2013. Induced seismicity and the O&G Industry. *In*: *Ground Water Protection Council, 2013 Underground Injection Control Conference, Sarasota, Florida, 22–24 January 2013*. http://www.gwpc.org/sites/default/files/event-sessions/Bull_Jeff.pdf. (accessed 4 January 2014)

CALDER, P.N. 1977. Perimeter blasting. *In*: *Pit Slope Manual, CANMET Report 77-14*. Canadian Center for Mineral and Energy Technology. Ottawa, ON, 60–82.

CARTER, P.G. & MILLS, D.A. 1976. Engineering geological investigations for the Kielder Tunnels. *Quarterly Journal of Engineering Geology*, **9**, 125–141.

COAL AUTHORITY 2004. Coal mining subsidence damage: A guide to claimants' rights. Coal Authority, Mansfield. http://coal.decc.gov.uk/assets/coal/whatwedo/coalminingsubsidencedamageaguidetoclaimantsrights.pdf. (accessed 4 January 2014)

DARRAH, T.H., VENGOSH, A., JACKSON, R.B., WARNER, N.R. & POREDA, R.J. 2014. Noble gases identify the mechanisms of fugitive gas contamination in drinking-water wells overlying the Marcellus and Barnett Shales. *Proceedings of the National Academy of Sciences of the United States of America*, **111**, 14076-14081. http://dx.doi.org/10.1073/pnas.1322107111

DAVIES, R.J., MATHIAS, S., MOSS, J., HUSTOFT, S. & NEWPORT, L. 2012. Hydraulic fractures: How far can they go? *Marine and Petroleum Geology*, **37**, 1–6.

DAVIES, R.J., FOULGER, G.R., MATHIAS, S., MOSS, J., HUSTOFT, S. & NEWPORT, L. 2013. Reply: Davies *et al.* (2012), Hydraulic fractures: How far can they go? *Marine and Petroleum Geology*, **43**, 519–521.

DECC 2013*a*. Energy Consumption in the UK (2013). *In*: *Domestic energy consumption in the UK between 1970 and 2012*. Department of Energy and Climate Change, London. https://www.gov.uk/government/uploads/system/uploads/attachment_data/file/65954/chapter_3_domestic_factsheet.pdf. (accessed 2 June 2014)

DECC 2013*b*. Onshore oil and gas exploration in the UK: Regulation and best practice. Department of Energy and Climate Change, London. https://www.gov.uk/government/uploads/system/uploads/attachment_data/file/265988/Onshore_UK_oil_and_gas_exploration_England_Dec13_contents.pdf. (accessed 10 May 2014)

DECC 2014. Fracking UK shale: Water. Department of Energy and Climate Change, London. https://www.gov.uk/government/uploads/system/uploads/attachment_data/file/277211/Water.pdf. (accessed 7 July 2014)

DE PATER, C.J. & BAISCH, S. 2011. Geomechanical study of Bowland Shale seismicity: Synthesis report. Cuadrilla Resources Ltd, Lichfield. http://www.shalegas-europe.eu/en/index.php/resources/library/environment-and-safety/44-geomechanical-study-of-bowland-shale-seismicity. (accessed 3 January 2014)

DONNELLY, L.J. 2006. A review of coal mining induced fault reactivation in Great Britain. *Quarterly Journal of Engineering Geology and Hydrogeology*, **39**, 5–50.

EATON, D.W., VAN DER BAAN, M., BIRKELO, B. & TARY, J.-B. 2014. Scaling relations and spectral characteristics of tensile microseisms: Evidence for opening/closing cracks during hydraulic fracturing. *Geophysical Journal International*, **196**, 1844–1857.

EAVES, T. & JONES, T.M. 1971. Cohesion and tensile strength of bulk solids. *Rheologica Acta*, **10**, 127–134.

ELLSWORTH, W.L. 2013. Injection-induced earthquakes. *Science*, **341**, 1225942, http://dx.doi.org/10.1126/science.1225942.

ENGLAND, A.H. & GREEN, A.E. 1963. Some two-dimensional punch and crack problems in classical elasticity. *Mathematical Proceedings of the Cambridge Philosophical Society*, **59**, 489–500.

ESHELBY, J.D. 1957. The determination of the elastic field of an ellipsoidal inclusion, and related problems. *Proceedings of the Royal Society of London, Series A*, **241**, 376–396.

FISHER, K. & WARPINSKI, N. 2012. Hydraulic-fracture-height growth: Real data. *Society of Petroleum Engineers, Productions and Operations Journal*, **27**, 8–19.

FOJTÍKOVÁ, L., VAVRYČUK, V., CIPICAR, A. & MADARÁS, J. 2010. Focal mechanisms of micro-earthquakes in the Dobrá Voda seismoactive area in the Malé Karpaty Mts. (Little Carpathians), Slovakia. *Tectonophysics*, **492**, 213–229.

FOX, J. 2010. *Gasland*. New Video Group, New York.

FRANKEL, A. & CLAYTON, R.W. 1986. Finite difference simulations of seismic scattering: Implications for the propagation of short-period seismic waves in the crust and models of crustal heterogeneity. *Journal of Geophysical Research*, **91**, 6465–6489.

FRANKEL, A. & WENNERBERG, L. 1987. Energy-flux model of seismic coda: Separation of scattering and intrinsic attenuation. *Bulletin of the Seismological Society of America*, **77**, 1223–1251.

GALE, J.F.W. & HOLDER, J. 2008. Natural fractures in the Barnett Shale: Constraints on spatial organization and tensile strength with implications for hydraulic fracture treatment in shale-gas reservoirs. *In*: *Proceedings of the 42nd U.S. Rock Mechanics Symposium and 2nd U.S.–Canada Rock Mechanics Symposium, 29 June–2 July 2008, San Francisco, California*. Curran Associates, Red Hook, NY, 243–251.

GAO, L., JING, Y. & LI, J. 2013. High frequency S wave envelope synthesis using a multiple nonisotropic scattering model: Application to aftershocks from the 2008 Wenchuan earthquake. *Earthquake Engineering and Engineering Vibration*, **12**, 185–194.

GEISER, P., LACAZETTE, A. & VERMILYE, J. 2012. Beyond 'dots in a box': An empirical view of reservoir permeability with tomographic fracture imaging. *First Break*, **30**, 63–69.

GOULTY, N.R. 2005. Emplacement mechanism of the Great Whin and Midland Valley dolerite sills. *Journal of the Geological Society, London*, **162**, 1047–1056.

GREEN, C.A., STYLES, P. & BAPTIE, B.J. 2012. Preese Hall shale gas fracturing: Review and recommendations for induced seismic mitigation. UK Government Department of Energy and Climate Change, London. https://www.gov.uk/government/uploads/system/uploads/attachment_data/file/48330/5055-preese-hall-shale-gas-fracturing-review-and-recomm.pdf. (accessed 3 January 2014)

GRIDWATCH 2014. *U.K. National Grid status*. http://www.gridwatch.templar.co.uk/. (accessed 3 January 2014)

GRIFFITH, A.A. 1924. The theory of rupture. *In*: BIEZENO, C.B. & BURGERS, J.M. (eds) *Proceedings of the First International Congress of Applied Mechanics, Delft, The Netherlands*. Technische Boekhandel en Drukkerij, Delft, 55–63.

HANKS, T.C. & KANAMORI, H. 1979. A moment magnitude scale. *Journal of Geophysical Research*, **84**, 2348–2350.

HEALY, J.H., RUBEY, W.W., GRIGGS, D.T. & RALEIGH, C.B. 1968. The Denver earthquakes. *Science*, **161**, 1301–1310.

HERRMANN, R.B., PARK, S.-K. & WANG, C.-Y. 1981. The Denver earthquakes of 1967–1968. *Bulletin of the Seismological Society of America*, **71**, 731–745.

HITZMAN, M.W., CLARKE, D.D., ET AL. 2013. *Induced Seismicity Potential in Energy Technologies*. National Academy of Sciences, Washington, DC. World Wide Web Address: http://www.nap.edu/catalog.php?record_id=13355. (accessed 3 January 2014)

HOLLAND, A. 2011. Examination of possibly induced seismicity from hydraulic fracturing in the Eola Field, Garvin County, Oklahoma. Oklahoma Geological Survey Open-File Report, OF1-2011. http://www.ogs.ou.edu/pubsscanned/openfile/OF1_2011.pdf. (accessed 3 January 2014)

HOUSE OF LORDS 2014. The Economic Impact on UK Energy Policy of Shale Gas and Oil. House of Lords Economic Affairs Committee, 3rd Report of Session 2013–14. HL Paper 172. Stationery Office, London. http://www.publications.parliament.uk/pa/ld201314/ldselect/ldeconaf/172/172.pdf. (accessed 8 May 2014)

HSIEH, P.A. & BREDEHOEFT, J.S. 1981. A reservoir analysis of the Denver earthquakes: A case of induced seismicity. *Journal of Geophysical Research*, **86**, 903–920.

IDE, S. & BEROZA, G.C. 2001. Does apparent stress vary with earthquake size? *Geophysical Research Letters*, **28**, 3349–3352.

IMECHE, 2011. Scottish Energy 2020? Institution of Mechanical Engineers, London. http://www.imeche.org/docs/default-source/events/IMechE_Scottish_Energy_Report.pdf?sfvrsn=0. (accessed 2 June 2014)

JACKSON, R.B., VENGOSH, A., ET AL. 2013. Increased stray gas abundance in a subset of drinking water wells near Marcellus shale gas extraction. *Proceedings of the National Academy of Sciences of the United States of America,* **110**, 11250–11255.

KANAMORI, H. 1977. The energy release in great earthquakes. *Journal of Geophysical Research*, **82**, 2981–2987.

KEILIS-BOROK, V.I. 1959. On estimation of the displacement in an earthquake source and of source dimensions. *Annali di Geofisica*, **12**, 205–214.

KERANEN, K.M., SAVAGE, H.M., ABERS, G.A., COCHRAN, E.S. & SUMY, D.F. 2013. Potentially induced earthquakes in Oklahoma, USA: Links between wastewater injection and the 2011 $M_w$ 5.7 earthquake sequence. *Geology*, **41**, 699–702.

KERR, R.A. 2013. Some earthquakes warn that they are about to strike. *Science*, **341**, 117–118.

KLOSE, C.D. 2007. Mine water discharge and flooding: A cause of severe earthquakes. *Mine Water and the Environment*, **26**, 172–180.

KLOSE, C.D. 2013. Mechanical and statistical evidence of the causality of human-made mass shifts on the Earth's upper crust and the occurrence of earthquakes. *Journal of Seismology*, **17**, 109–135.

KUSZNIR, N.J., ASHWIN, D.P. & BRADLEY, A.G. 1980. Mining induced seismicity in the North Staffordshire coalfield, England. *International Journal of Rock Mechanics and Mining Sciences & Geomechanics Abstracts*, **17**, 45–55.

KWIATEK, G. & BEN-ZION, Y. 2013. Assessment of P and S wave energy radiated from very small shear-tensile seismic events in a deep South African mine. *Journal of Geophysical Research: Solid Earth*, **118**, 3630–3641.

LACAZETTE, A. & GEISER, P. 2013. Comment on Davies *et al.* 2012—Hydraulic fractures: How far can they go? *Marine and Petroleum Geology*, **43**, 516–518.

LAY, T. & WALLACE, T.C. 1995. *Modern Global Seismology*. Academic Press, New York.

LI, V.C. 1984. Estimation of *in-situ* hydraulic diffusivity of rock masses. *Pure and Applied Geophysics*, **122**, 545–559.

LUNN, R.J., SHIPTON, Z.K. & BRIGHT, A.M. 2008. How can we improve estimates of bulk fault zone hydraulic properties? *In*: WIBBERLEY, C.A.J., KURZ, W., IMBER, J., HOLDSWORTH, R.E. & COLLETTINI, C. (eds) *The Internal Structure of Fault Zones: Implications for Mechanical and Fluid-Flow Properties*. Geological Society, London, Special Publications, **299**, 231–237.

MAIR, R., BICKLE, M., *ET AL.* 2012. Shale gas extraction in the UK: a review of hydraulic fracturing. Royal Society, London and Royal Academy of Engineering, London. http://royalsociety.org/uploadedFiles/Royal_Society_Content/policy/projects/shale-gas/2012-06-28-Shale-gas.pdf. (accessed 4 January 2014)

MARTINEAU, D.F. 2007. History of the Newark East field and the Barnett Shale as a gas reservoir. *AAPG Bulletin*, **91**, 399–403.

MUHURI, S.K., DEWERS, T.A., SCOTT, T.E., JR. & RECHES, Z. 2003. Interseismic fault strengthening and earthquake-slip instability: Friction or cohesion? *Geology*, **31**, 881–884.

NCHRP 1999. *Mitigation of nighttime construction noise, vibrations, and other nuisances: A synthesis of highway practice*, National Cooperative Highway Research Program, Washington, DC.

ORIARD, L.L. 1972. Blasting operations in the urban environment. *Bulletin of the Association of Engineering Geologists,* **9**, 27–46.

ORIARD, L.L. 2002. *Explosives Engineering, Construction Vibrations and Geotechnology*. International Society of Explosives Engineers, Cleveland, OH.

RAMSEY, J.M. & CHESTER, F.M. 2004. Hybrid fracture and the transition from extension fracture to shear fracture. *Nature*, **428**, 63–66.

RANKINE, W.J.M. 1843. On the causes of the unexpected breakage of the journals of railway axles, and on the means of preventing such accidents by observing the law of continuity in their construction. *Minutes of the Proceedings of the Institution of Civil Engineers*, **2**, 105–107.

RANKINE, W.J.M. 1858. *A Manual of Applied Mechanics*. Richard Griffin, Glasgow.

RECHES, Z. 1999. Mechanisms of slip nucleation during earthquake. *Earth and Planetary Science Letters*, **170**, 475–486.

RICE, J.R. 1980. Elastic wave emission from damage processes. *Journal of Nondestructive Evaluation*, **1**, 215–224.

RICHTER, C.F. 1958. *Elementary Seismology*. Freeman, San Francisco, CA.

SATO, H. & FEHLER, M. 1998. *Seismic Wave Propagation and Scattering in the Heterogeneous Earth*. Springer, New York.

SEEBER, N. 2002. Mechanical pollution. *Seismological Research Letters*, **73**, 315–317.

SHAW, B.E. 2009. Constant stress drop from small to great earthquakes in magnitude-area scaling. *Bulletin of the Seismological Society of America*, **99**, 871–875.

SHI, Z. & BEN-ZION, Y. 2009. Seismic radiation from tensile and shear point dislocations between similar and dissimilar solids. *Geophysical Journal International*, **179**, 444–458.

ŠÍLENÝ, J., HILL, D.P., EISNER, L. & CORNET, F.H. 2009. Non-double-couple mechanisms of microearthquakes induced by hydraulic fracturing. *Journal of Geophysical Research*, **114**, B08307, http://dx.doi.org/10.1029/2008JB005987.

SIMONSON, E.R., ABOU-SAYED, A.S. & CLIFTON, R.J. 1978. Containment of massive hydraulic fractures. *Society of Petroleum Engineers Journal*, **18**, 27–32.

SISKIND, D.E., STAGG, M.S., KOPP, J.W. & DOWDING, C.H. 1980. *Structure response and damage produced by ground vibration from surface mine blasting*. US Bureau of Mines, Report of Investigations, **8507**.

SNEDDON, I.N. 1951. *Fourier Transforms*. McGraw–Hill, New York.

SOLUM, J.G., DAVATZES, N.C. & LOCKNER, D.A. 2010. Fault-related clay authigenesis along the Moab Fault: Implications for calculations of fault rock composition and mechanical and hydrologic fault zone properties. *Journal of Structural Geology*, **32**, 1899–1911.

SONG, F. & TOKSÖZ, M.N. 2011. Full-waveform based complete moment tensor inversion and source parameter estimation from downhole microseismic data for hydrofracture monitoring. *Geophysics*, **76**, WC103–WC116.

SONG, F., WARPINSKI, N.R. & TOKSÖZ, M.N. 2014. Full-waveform based microseismic source mechanism studies in the Barnett Shale: Linking microseismicity to reservoir geomechanics. *Geophysics*, **79**, KS109–KS126.

STAGG, M.S., SISKIND, D.E., STEVENS, M.G. & DOWDING, C.H. 1980. *Effects of repeated blasting on a wood frame house*. US Bureau of Mines, Report of Investigations, **8896**.

TOKSÖZ, M.N. & JOHNSTON, D.H. 1981. *Seismic Wave Attenuation*. Society of Exploration Geophysicists, Tulsa, OK.

TRAN, D.T., ROEGIERS, J.-C. & THIERCELIN, M. 2010. Thermally-induced tensile fractures in the Barnett Shale and their implications to gas shale fracability. *In*: *Proceedings of the 44th US Rock Mechanics Symposium and 5th U.S.–Canada Rock Mechanics Symposium, 27–30 June 2010, Salt Lake City, Utah*. Curran Associates, Red Hook, NY, 1228–1241.

UKOOG 2013. UK Onshore Shale Gas Well Guidelines: Issue 1, February 2013; Exploration and appraisal phase. United Kingdom Onshore Operators' Group, Cranbrook. https://www.gov.uk/government/uploads/system/uploads/attachment_data/file/185935/UKOOGShaleGas WellGuidelines.pdf. (accessed 3 January 2014)

VAN DER ELST, N.J., SAVAGE, H.M., KERANEN, K.M. & ABERS, G.A. 2013. Enhanced remote earthquake triggering at fluid-injection sites in the midwestern United States. *Science*, **341**, 164–167.

VAN DER MEER, J.J.M., KJÆR, K.H., KRÜGER, J., RABASSA, J. & KILFEATHER, A.A. 2009. Under pressure: Clastic dykes in glacial settings. *Quaternary Science Reviews*, **28**, 708–720.

VARGA, R., PACHOS, A., HOLDEN, T., PENDREL, J., LOTTI, R., MARINI, I. & SPADAFORA, E. 2012. Seismic inversion in the Barnett Shale successfully pinpoints sweet spots to optimize wellbore placement and reduce drilling risks. *In*: *Proceedings of the 2012 Society of Exploration Geophysicists Annual Meeting, 4–9 November 2012, Las Vegas, Nevada*. Curran Associates, Red Hook, NY, 4023–4027.

VAVRYČUK, V. 2011. Tensile earthquakes: Theory, modeling, and inversion. *Journal of Geophysical Research*, **116**, B12320, http://dx.doi.org/10.1029/2011JB008770.

WALD, D.J., QUITORIANO, V., HEATON, T.H. & KANAMORI, H. 1999. Relationships between peak ground acceleration, peak ground velocity, and modified Mercalli intensity in California. *Earthquake Spectra*, **15**, 557–564.

WALTER, W.R. & BRUNE, J.N. 1993. Spectra of seismic radiation from a tensile crack. *Journal of Geophysical Research*, **98**, 4449–4459.

WALTHAM, A.C. 2009. *Foundations of Engineering Geology*, 3rd edn. Spon, London.

WARPINSKI, N.R. 2013. Understanding hydraulic fracture growth, effectiveness, and safety through microseismic monitoring. *In*: BUNGER, A.P., MCLENNAN, J. & JEFFREY, R. (eds) *Effective and Sustainable Hydraulic Fracturing*. InTech, Rijeka, Croatia, 124–135. http://cdn.intechopen.com/pdfs-wm/44586.pdf. (accessed 12 May 2014)

WESTAWAY, R. 2002. Seasonal seismicity of northern California before the great 1906 earthquake. *Pure and Applied Geophysics*, **159**, 7–62.

WESTAWAY, R. 2006. Investigation of coupling between surface processes and induced flow in the lower continental crust as a cause of intraplate seismicity. *Earth Surface Processes and Landforms*, **31**, 1480–1509.

WESTAWAY, R. & SMITH, R. 1989. Strong ground motion in normal faulting earthquakes. *Geophysical Journal*, **96**, 529–559.

WHIFFEN, A.C. & LEONARD, D.R. 1971. *A survey of traffic-induced vibrations*. Transport and Road Research Laboratory, Laboratory Report LR418. Transport and Road Research Laboratory, Crowthorne, Berkshire.

WU, Y.-M., HSIAO, T.-L. & TENG, N.C. 2004. Relationship between peak ground acceleration, peak ground velocity, and intensity in Taiwan. *Natural Hazards*, **32**, 357–373.

YOUNGER, P.L. 2014. Hydrogeological challenges in a low-carbon economy. *Quarterly Journal of Engineering Geology and Hydrogeology*, **47**, 7–27. http://dx.doi.org/10.1144/qjegh2013-063